Renewable and Sustainable Energy Reviews 32 (2014) 591–610

Contents lists available at ScienceDirect

Renewable and Sustainable Energy Reviews

journal homepage: www.elsevier.com/locate/rser

A review on high temperature thermochemical heat energy storage

P. Pardo [a], A. Deydier [a], Z. Anxionnaz-Minvielle [a,*], S. Rougé [a], M. Cabassud [b,c], P. Cognet [b,c]

[a] CEA, LITEN, LETH, 17 rue des Martyrs, 38054 Grenoble, France
[b] Université de Toulouse; INPT, UPS, Laboratoire de Génie Chimique, 4, Allée Emile Monso, F-31432 Toulouse, France
[c] CNRS, Laboratoire de Génie Chimique, F-31432 Toulouse, France

ARTICLE INFO

Article history:
Received 9 December 2011
Received in revised form
18 October 2013
Accepted 19 December 2013
Available online 5 February 2014

Keywords:
Thermal Energy Storage (TES)
Thermochemical
Reversible reactions
Concentrated solar plant (CSP)

ABSTRACT

Solar thermal energy represents an increasingly attractive renewable source. However, to provide continuous availability of this energy, it must be stored. This paper presents the state of the art on high temperature (573–1273 K) solar thermal energy storage based on chemical reactions, which seems to be the most advantageous one for long-term storage. The paper summarizes the numerical, experimental and technological studies done so far. Each system is described and the advantages and drawbacks of each reaction couple are considered.

Contents

* Corresponding author.
E-mail address: zoe.minvielle@cea.fr (Z. Anxionnaz-Minvielle).

1364-0321/$ - see front matter
http://dx.doi.org/10.1016/j.rser.2013.12.014

Nomenclature

A	product A [dimensionless]
B	Product B [dimensionless]
C	product C [dimensionless]
Cp	specific heat of the media, kWh kg^{-1} K^{-1} or kJ kg^{-1} K^{-1}
D_m	gravimetric energy density, kWh kg^{-1}
D_v	volumetric energy density, kWh m^{-3}
K	thermodynamic equilibrium constant [dimensionless]
L	latent enthalpy, kWh kg^{-1}
M	mass of media, kg
n_A	mol number of product A, mol
P_u	useful power, kW
Q	thermal energy stored, kWh
T	temperature of the system, K
T^*	turning temperature, K
V	volume of media, m^{-3}
ΔH_r	reaction enthalpy, kWh mol^{-1} or kJ mol^{-1}
Δt	time difference, s
ΔT	temperature difference, K
ΔS_r	reaction entropy kJ K^{-1}
η	thermal efficiency [dimensionless]
+	advantages level of importance (+++high, ++medium, +low) [dimensionless]
−	drawbacks level of importance (−−− high, −− medium, −low) [dimensionless]

1. Introduction

The use of renewable energy is essential today to decrease the consumption of fossil resources and to decrease the production of carbon dioxide partly responsible for the greenhouse effect [1]. Solar energy constitutes an attractive source of energy because it is both free and endless. It can be converted into electricity by means of a concentrated solar plant (CSP) composed of four elements: a concentrator, a receiver, a transport media system and a power conversion machine. However, the major drawback of this energy is its intermittence. One solution is to develop thermal energy storage (TES) systems, which will store heat during the sunshine periods and release it during the periods of weak or no solar irradiation. A CSP equipped with a TES system would continuously supply electricity. Thus, the development of an efficient and cost-effective TES system is crucial for the future of this technology.

At the moment, three kinds of TES systems are known: the sensible heat storage, the latent heat storage and the thermochemical heat storage [1,2]. Sensible heat storage systems are the most mature technologies. They have been and are still being used in industrial plants, most notably in Spain, with the PS10 and PS20 projects (2007 and 2009) or the Andasol 1 and 2 plants (2008), but also in the USA, e.g. with Solar One (1982) [2]. Among the other techniques, thermochemical heat storage seems to be a valid option to be used as a TES system [3,4]. However, in order to be efficient and cost-effective, the appropriate reversible chemical reactions have to be identified [5]. Recently, two reviews focusing on low temperature (273–573 K) TES systems based on chemical reactions have been published. They respectively concern long-term sorption solar energy storage [6] and chemical heat pump technologies and their applications [7]. Cot-Gores et al. [8] also published a state-of-the-art on sorption and chemical reaction processes for TES application and some of the high temperature reactions are listed in the Felderhoff et al. article [9].

The purpose of this work is to provide a state-of-the-art of the thermochemical heat storage solutions, focusing on temperatures comprised between 573 K and 1273 K. General definitions as well as the disciplines involved in the development of a TES system are detailed. The experimental facilities at pilot or laboratory scales and their applications are reviewed and described. The systems have been classified according to their reaction family (carbonation, hydration, oxidation…) since they often share the same advantages and drawbacks. The main data have been compiled in 2 graphs (densities versus temperature) and a general table which summarizes the literature data about reversible reactions studied for thermochemical storage applications is given.

2. Thermal energy storage: definitions

Thermal storage systems have to be used to correct the existing mismatch between the discontinuous solar energy supply and the continuous electricity consumption [1]. They involve at least three steps: heat charging, storage and discharging. Three mechanisms of storing thermal energy exist. They are described below.

In sensible heat storage systems, during the charging step, solar energy is used to heat a fluid or a solid medium, thus, increasing its energy content. Then, the medium is stored at the charging step temperature. When this energy is released (discharging step), the medium temperature decreases. The sensible heat stored is associated with this increase or decrease of temperature. The thermal energy stored by sensible heat can be expressed as

$$Q = mCp\Delta T$$

Where m is the mass of the material (kg), Cp is the specific heat over the temperature range operation (kJ kg^{-1} K^{-1}) and ΔT is the temperature difference (K). Two reviews list the materials and the works done for high temperature thermal energy storage based on sensible heat [1,2].

In latent heat storage, during the charging step, solar energy can be used as the heat source that initiates a phase change. Then, the medium is stored at the charging step temperature into its new phase. When this energy is released (discharging step), the medium phase changes into the first state. The latent heat stored is associated with this phase change. The thermal energy stored in phase change material can be expressed as:

$$Q = mL$$

Where m is the mass of the material (kg) and L is the latent heat of the material (kJ kg^{-1}).Many publications deal with latent TES systems. For instance, a review lists the materials, the heat transfer analysis and the applications [10]; another one lists both the materials and the works done for high temperature thermal energy storage based on phase change material (PCM) [11].

The reactions involved in the thermochemical heat storage system are reversible ones:

$$A + \Delta H_r \Leftrightarrow B + C$$

Heat is stored during the endothermic reaction step and released during the exothermic one. The thermochemical heat stored is linked to the reaction enthalpy. During the charging step, thermal energy is used to dissociate a chemical reactant (A), into products (B) and (C). This reaction is endothermic. During the releasing step, the products of the endothermic reaction (B and C) are mixed together and react to form the initial reactant (A). This reaction is exothermic and releases heat. The products of both

reactions can be stored either at ambient temperature or at working temperature. The thermal energy stored in thermochemical material can be expressed as:

$$Q = n_A \Delta H_r$$

Where n_A is the mol number of the reactant A (mol) and ΔH_r is the reaction enthalpy (kWh mol_A^{-1}). The simplified scheme of a TES system based on chemical reactions is presented on Fig. 1.

2.1. Energy density

In this paper, the energy density is assessed from the endothermic reactant (A) mass or volume. The energy density can be defined in two ways. The first one and also the most used is the volumetric energy density, expressed as:

$$D_v = Q/V$$

Where D_v is the volumetric energy density (kWh m^{-3}), Q is the stored thermal energy (kWh) and V is the storage material volume (m^3).

In case of G/S reactions, if the A product is a gas, the temperature and pressure conditions have to be specified. If the A product is a solid, it is important to know which property among the true density, the apparent density or the bulk density is being used. True density is defined as the material density without porosity. Apparent density is defined as the average density of the material and includes the volume of pores within the particle boundary. Bulk density is defined as the density of the packed bed of particles. Once this property is known, the volume can be assessed. To be rigorous, the volumetric energy density should be calculated with the biggest volume or the installation volume.

The second definition is that of gravimetric energy density, expressed as

$$D_m = Q/m$$

Where D_m is the mass energy density (kWh kg^{-1}), Q is the stored thermal energy (kWh) and m is the storage material mass (kg).

Both energy densities are important in order to estimate the size and the cost of the TES system.

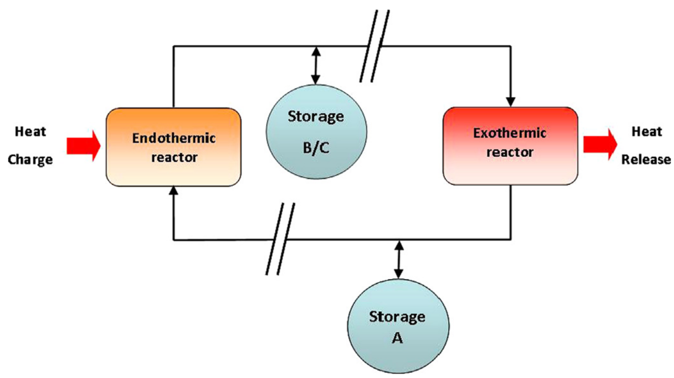


Fig. 1. Simplified scheme of a TES system based on chemical reactions.

Table 1
Characteristics and comparison of the thermal energy storage systems [1].

	Sensible heat storage system	Latent heat storage system	Thermochemical storage system
Energy density			
Volumetric density	Small ~50 kWh m^{-3} of material	Medium ~100 kWh m^{-3} of material	High ~500 kWh m^{-3} of reactant
Gravimetric density	Small ~0.02–0.03 kWh kg^{-1} of material	Medium ~0.05–0.1 kWh kg^{-1} of material	High ~0.5–1 kWh kg^{-1} of reactant
Storage temperature	Charging step temperature	Charging step temperature	Ambient temperature
Storage period	Limited (thermal losses)	Limited (thermal losses)	Theoretically unlimited
Transport	Small distance	Small distance	Distance theoretically unlimited [12]
Maturity	Industrial scale	Pilot scale	Laboratory scale
Technology	Simple	Medium	Complex

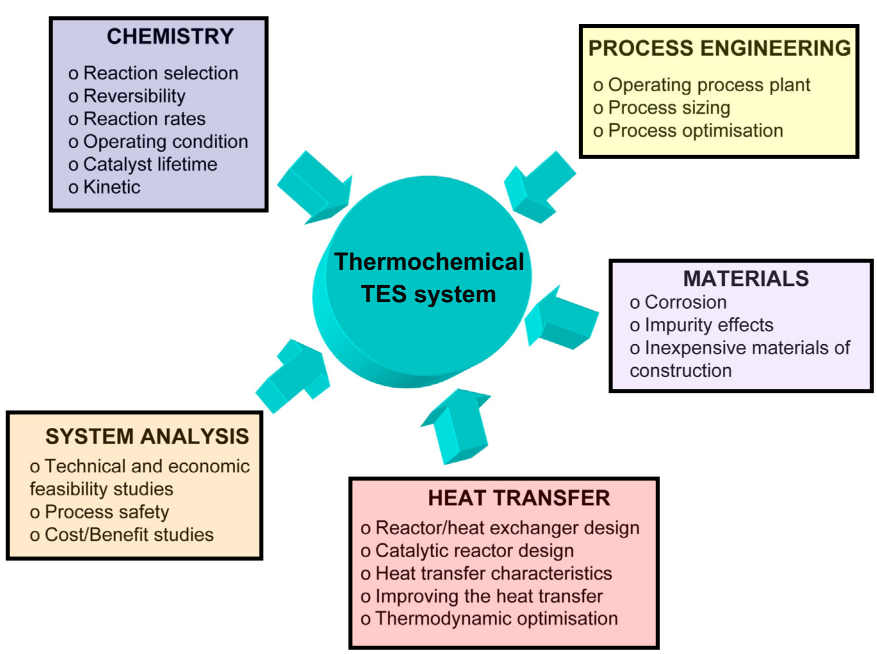


Fig. 2. Technical disciplines necessary to the development of a TES system based on chemical reactions [4].

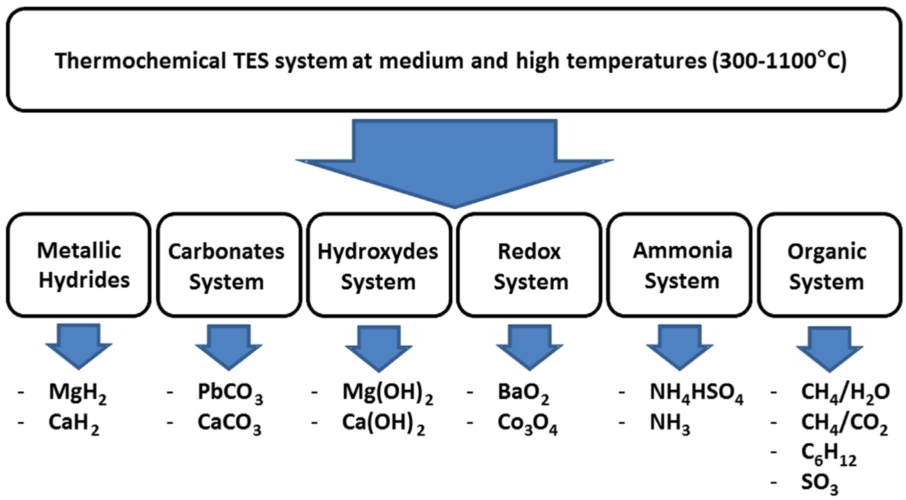


Fig. 3

2.2. Comparison of different TES systems

To compare the three different TES systems, six parameters are considered: the energy density, the storage temperature, the storage period, the material transportation possibility, the maturity of the TES system and the complexity of associated technologies.

The characteristic data of each storage system are given in Table 1.

Thermochemical storage systems have several advantages. Their energy densities are 5 to 10 times higher than latent heat storage system and sensible heat storage system respectively. Both storage period and transport are theoretically unlimited because there is no thermal loss during storage, as products can be stored at ambient temperature. Thus, these systems are promising to store solar thermal energy during a long-term period. Nevertheless, unlike sensible and latent heat storage systems there is only little experience feedback on thermochemical storage.

3. State-of-the-art on solar thermal energy storage based on chemical reactions

3.1. Technical disciplines and skills for developing a thermochemical TES system

Thermochemical TES systems are still at a very early stage of development. Most of the studies are done at laboratory scale. Considerable amount of time, money and efforts are required before a commercially viable system becomes operational. The technical disciplines identified by Garg et al. [4] to develop a thermochemical TES system are updated and presented on Fig. 2.

Usually, the first step to develop a thermochemical TES system is the selection of the reaction and the study of its chemical characteristics such as the reversibility, the rate of reaction, the operating conditions (P and T) and the kinetic properties. Wentworth and Chen [5] reported that the following criteria ought to be respected for choosing the most suitable chemical reaction in the thermochemical TES system:

- The endothermic reaction used for heat storage should occur at a temperature lower than 1273 K.
- The exothermic reaction used to recover heat should occur at a temperature higher than 773 K.
- Large enthalpies of reaction and a product of small molar volume are required to maximize the storage capacity ($\sim$500 kWh m^{-3}).
- Both reactions should be completely reversible, with no side reactions, and have high yields in order to use the materials over a long period of time.
- Both reactions should be fast enough so that the absorption of solar energy and heat release can be carried out rapidly.
- The chemical compounds of both reactions should be easily handleable.
- When stored, the chemical compounds should not react with their environment.
- Experiment feedback on the reaction is required to use a well-known chemical process.
- Low costs should be required.

Some papers list reversible reactions which can be used for a TES system [3–5,13]. Usually, their characteristics are reactant family, reaction enthalpy and turning temperature. For a reversible reaction of the type $aA \Leftrightarrow bB + cC$ and a given pressure, the turning temperature T^* is defined as the temperature at which the reaction rate constant K is equal to 1, and is approximated as $T^* = \Delta H_r / \Delta Sr$. As $K < 1$ when $T > T^*$ and $K > 1$ for $T < T^*$ [4,5]. The turning temperature T^* may help knowing the required temperature conditions to carry out both endothermic and exothermic reactions [4,5]. The study of chemistry properties allows the determination of the required operating conditions. Then, the chemical engineering work can start with the choice of the reactor technology, the material, the operating process plant design and the system analysis.

The following state-of-the-art underlines the different reactions which were or are studied for a thermochemical TES plant. These reactions are classified in six systems which are illustrated in Fig. 3.

3.2. Hydrogen systems: metallic hydrides

The general form of a reaction using a metal M, is

$$MH_n + \Delta H_r \Leftrightarrow M + n/2H_2$$

Usually, the reversible metallic hydride reactions are used to store hydrogen. In fact, one of the first research works were performed in the automotive industry for the hydrogen motor [14]. They led to the design of reactor before being used for heat pumps [15] and, in the beginning of the 90s, for the thermal energy storage [14].

Three metallic hydrides have been studied for the thermal energy storage in concentrated solar plants: lithium hydride (LiH) for the TES using its energy of phase change, calcium hydride (CaH_2) for heat storage at high temperature between 1223 and 1373 K and magnesium hydride (MgH_2) for both applications [16].

We only focus on the reaction involving magnesium hydride studied for a thermochemical TES application [17]. The reaction is written as

$$MgH_{2(s)} + \Delta H_r \Leftrightarrow Mg_{(s)} + H_{2(g)} \quad \text{with } \Delta H_r = 75 \text{ kJ mol}^{-1}.$$

The working temperatures range between 523 and 773 K with a hydrogen partial pressure between 1 and 100 bar. The knowledge of the H_2 dissociation (equilibrium) pressure as a function of temperature is of fundamental importance for the use of MgH_2/Mg couple as storage system (Fig. 4).

In the beginning of the 90s, the first research works start with the magnesium hydride [17] because of its high capacity of hydrogen storage (7.7 wt%) [16]. Nevertheless, using magnesium hydride involves major problems like slow kinetics and transfer limitations for large quantities of products. A paper reviews the works done for TES application [18]. In order to improve the rate of chemical reactions, the Mg powder was doped with a commercial Ni powder (4–10 wt%) and a Fe-powder (50 mol%). More than 1000 cycles were achieved with the Mg–Ni mixed powder, but a sintering phenomenon occurred. With the Mg_2FeH_6 powder, this phenomenon did not occur. 600 cycles were achieved without any drop in hydrogen capacity and the working pressure was lower than the working pressure for the pure material.

The Max-Planck institute designed and built three prototypes [18]: a steam generator (Fig. 5), a thermochemical solar plant (Fig. 6) and a solar cooking and cooling device.

The steam generator involves a MgH_2/Mg heat storage. The volume of the pressure vessel, closed to 20 L, is filled with a magnesium powder doped with a Ni powder (14.5 kg). A H_2 permeable tube set in the centre of the pressure vessel allows the hydrogen supply and the hydrogen recovery. Pressurized water flowing in a helical tube is set into the metallic hydride for the heat recovery and the vapour generation. The endothermic reaction can be implemented with a ribbon heater sealed around the pressure vessel. The hydrogen produced during the endothermic reaction is stored in six commercial vessels. The operating conditions are at a maximal pressure of 50 bar, a maximal temperature of 723 K and a maximal power of 4 kW.

The thermochemical solar plant is composed of a solar radiation concentrator, a cavity radiation receiver, a Stirling engine, a hydrogen tank pressure, a heat exchanger and a MgH_2/Mg storage device. The operating temperatures range between 623 K and 723 K. During the sunshine periods, electricity is produced and heat is stored by dissociating MgH_2. During the periods of weak or no solar irradiation, the hydrogen stored is supplied to the reactor to produce heat. Then, the heat is converted into electricity by the Stirling engine.

Table 2 presents the advantages and the drawbacks of the MgH_2/Mg system as a thermochemical TES system.

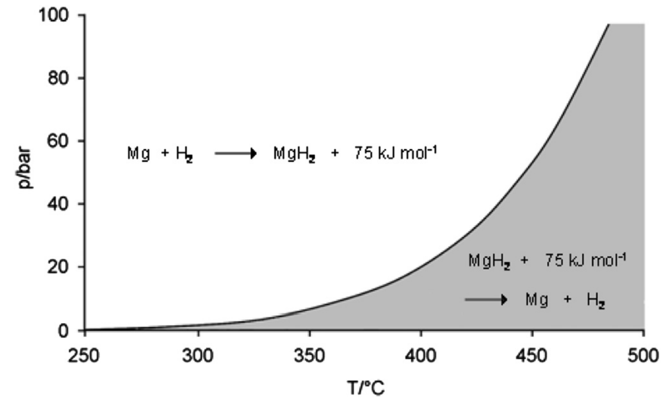


Fig. 4. Dissociation pressure curve of MgH_2 [13].

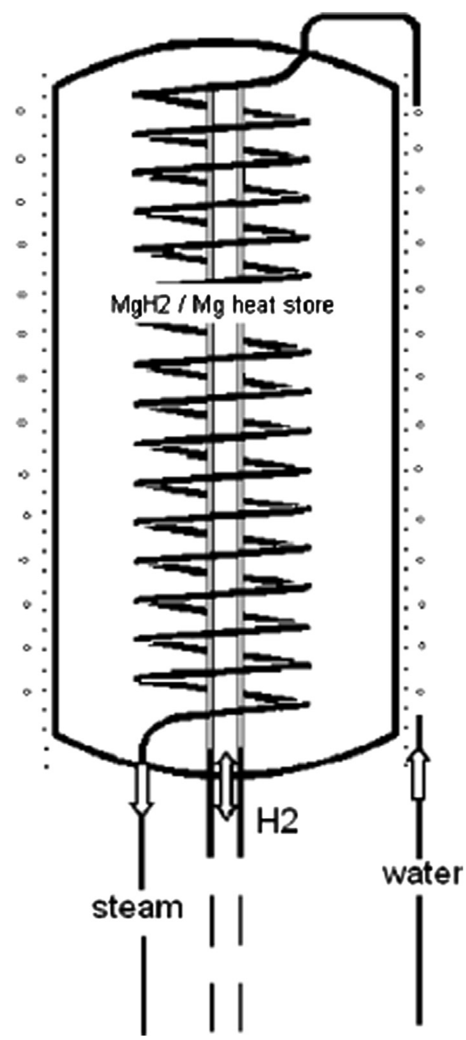


Fig. 5. Steam generator process based on MgH_2 [13].

3.3. Carbonate systems

The general reaction form is

$$MCO_{3(s)} + \Delta H_r \Leftrightarrow MO_{(s)} + CO_{2(g)}$$

Usually, these reactions occur at high temperature ($T > 723$ K). The calcination/carbonation reactions are driven by the CO_2 partial pressure and the temperature of the system. Two reversible reactions, the calcite and the cerrusite calcination/carbonation, were studied for a TES application. Today, most studies focus on the CO_2 sequestration with calcium carbonate [19].

3.3.1. Calcite calcination/carbonation

The reaction is

$$CaCO_{3(s)} + \Delta H_r \Leftrightarrow CaO_{(s)} + CO_{2(g)} \quad \text{with } \Delta H_r = 178 \text{ kJ mol}^{-1}.$$

The reversibility of the reaction can be used for a TES system application, for CO_2 sequestration or for limestone production. The working temperatures range between 973 and 1273 K with CO_2 partial pressure between 0 and 10 bar.

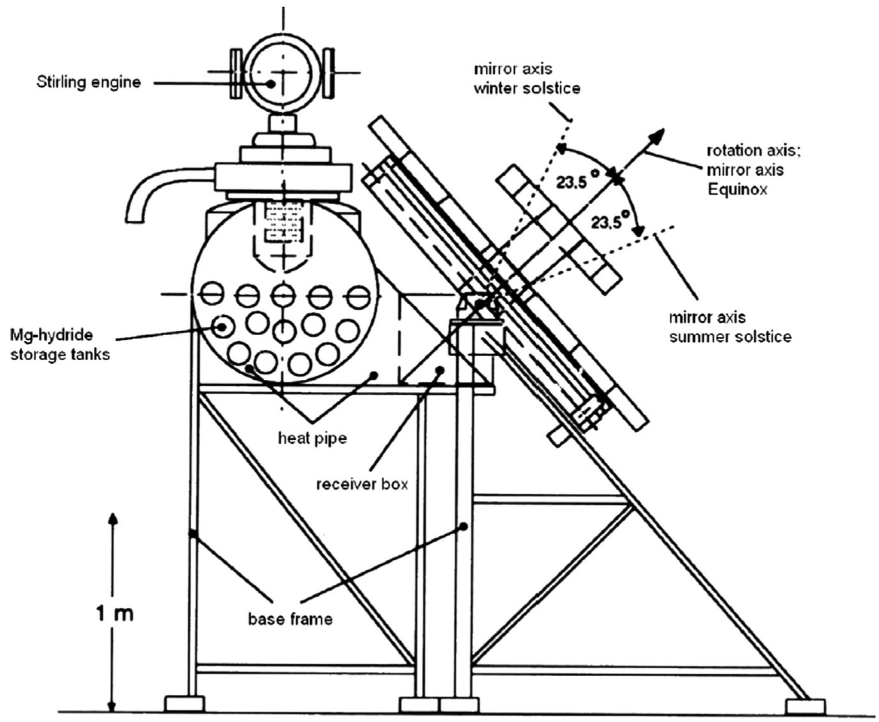


Fig. 6. Thermochemical solar plant [13].

Table 2
Advantages and drawbacks of the MgH_2/Mg system.

Reaction	Advantages	Drawbacks
$MgH_2 + \Delta H_r \Leftrightarrow Mg + H_2$	• Reversibility of the reaction (600 cycles) ++ • No by-product ++ • Product separation (Gas-solid) ++ • Experiment feedback +	• H_2 storage - • Slow reaction kinetics --- • Need of Fe- or Ni-doping -- • Sintering -- • Operating pressure (50–100 bar) --- • Heat transfer (solid/wall) ---

In the mid 70s, Barker [20] suggests to use this reaction for energy storage. His work focuses on the reversibility of the reaction. Many problems are observed with a 10 μm particle size powder due to the loss of specific surface. Indeed, a passivation layer is created during the carbonation and leads to a reaction limitation by decrease of the CO_2 diffusion in the particles. In order to solve this limitation, submicron particles have been used to avoid diffusion problems and finally to improve the reaction reversibility. While the material conversion reaches 93%, another problem arises. The volumetric energetic density of the product does not exceed 10% of the theoretical value of 35.3 kWh m^{-3} [21]. This huge decrease comes from the diminution of the density of the product in bulk.

At the beginning of the 80s, the calcination reaction is operated in two technologies of reactor: a fluidized bed in a batch mode (Fig. 7) and a continuous rotary kiln (Fig. 8) [22]. The fluidized bed works at a temperature between 873 and 1573 K with a solar furnace useful power of 1,4 kW.

A total conversion of $CaCO_3$ is reached. The thermal efficiency, defined as the ratio between the sum of the sensible energy and the reaction energy over the useful power given to the material during Δt, is between 20 and 40%. It is expressed as

$$\eta = (mCp\Delta T + n\Delta H_r)/(\Delta t P_u)$$

Where η is the thermal efficiency ([-]), m is the initial mass of the reactant A (kg), Cp is the specific heat over the temperature range operation (kJ kg^{-1} K^{-1}), ΔT is the temperature difference (K), n is the mol number of reactant A (mol), ΔHr is the reaction enthalpy (kJ mol^{-1}), Δt is the time difference (s) and P_u is the useful power (kW).

The rotary kiln (see Fig. 8) works at a temperature between 873 and 1573 K with a solar furnace useful power of 1.4 kW and is inclined 5° to the horizontal. A maximal conversion of 60% of $CaCO_3$ is experimentally reached with thermal efficiencies ranging from 10% to 30% [22,23]. Here, the residence times reached in the reactor are included between 20 and 120 s for rotary speed from 4 to 25 tr min^{-1}.

In order to improve the energetic efficiency of the reactors, Flamant [22] identifies the main causes of thermal losses and suggests some technological improvements on both the fluidization distributor and the cooling system of the rotary kiln. According to these proposals, Foro [25] develops an annular continuous fluidized reactor with an electrical power of 3 kW and 1 kW of useful power. He also demonstrates the thermal decomposition feasibility in the fluidized bed.

After many years without surveys, Kyaw et al. [26] realise a thermogravimetric study and suggest some new concepts for the storage system [13]. A conceptual flow diagram of $CaO–CO_2$

energy storing system is evaluated [26]. Three ways are used to store CO_2:

- a compressor and a tank;
- a carbonation reaction with MgO; and
- an adsorption reaction with zeolite.

The $CaO–CO_2–MgO$ system was the best system to convert heat energy at 773 K to temperatures around 1273 K. The $CaO–CO_2$ compressor system was the most suitable for storing and delivering thermal energy at the same temperature. The efficiency of $CaO–CO_2$-zeolite systems was strongly governed by the adsorption power of the zeolite.

Aihara et al. [27] improved the reversibility of the reaction by doping the material with titanium oxide ($CaTiO_3$). A thermogravimetric study was done and showed a stabilisation of the reversibility and no sintering. 10 cycles have been reached without loss of reversibility and with a global conversion rate of 65%. The operating conditions for the carbonation and the calcination were respectively 1023 K in nitrogen atmosphere and 1023 K with a gas mixture of $N_2–CO_2$ containing 20% of CO_2.

Meier et al. [24] developed a new solar reactor based on the technology of the rotary kiln (Fig. 8). The objective was to produce calcium oxide from limestone with an available power of 10 kW. The experiments have been done with 1 to 5 mm particles size and a conversion rate of 90–98% has been reached with a thermal efficiency of 20%.

Table 3 presents the advantages and the drawbacks of the $CaO/CaCO_3$ system as the thermochemical TES system.

3.3.2. Cerrusite calcination/carbonation

The reaction scheme is

$$PbCO_{3(s)} + \Delta H_r \Leftrightarrow PbO_{(s)} + CO_{2(g)} \quad \text{with } \Delta H_r = 88 \text{ kJ mol}^{-1}.$$

This reaction was studied for chemical heat pump applications [28–30] in order to be combined with the $CaCO_3/CaO$ system. The authors give operating temperatures from 573 to 1730 K with partial pressure of CO_2 included between 0 and 1 bar. A thermogravimetric analysis of the $PbCO_3/PbO/CO_2$ system was done to study the equilibrium relationship, the reaction reversibility (7 cycles of carbonation without loss of reactivity were achieved) and the kinetics of the reaction system [29]. The following mechanism of the decomposition reaction has been proposed:

Step A: $2PbCO_3 = Pb \cdot PbCO_3 + CO_2$
Step B: $3(PbO \cdot PbCO_3) = 2(2PbO \cdot PbCO_3) + CO_2$
Step C: $2PbO \cdot PbCO_3 = 3PbO + CO_2$

A packed bed reactor which combined PbO and CaO was built to study the thermal storage performance of the chemical heat pump [30]. The authors showed that the heat released by carbonation of CaO was measured experimentally up to 1143 K under a reaction pressure up to 1 atm.

Table 4 presents the advantages and the drawbacks of the $PbO/PbCO_3$ system as thermochemical TES system.

3.4. Hydroxide systems

The general reaction scheme is

$$M(OH)_{2(s)} + \Delta H_r \Leftrightarrow MO_{(s)} + H_2O_{(g)}$$

These reactions occur at medium temperature, usually $523 < T < 723$ K. The H_2O partial pressure and the temperature drive the hydration/dehydration reactions. Fig. 9 shows some of couples which could be used for a thermochemical TES application. Two reversible reactions were studied for a TES application [3,4]. These reactions are $MgO/Mg(OH)_2$ and $CaO/Ca(OH)_2$ hydration/dehydration.

3.4.1. Hydration/dehydration of magnesium oxide

The reaction is

$$Mg(OH)_{2(s)} + \Delta H_r \Leftrightarrow MgO_{(s)} + H_2O_{(g)} \quad \text{with } \Delta H_r = 81 \text{ kJ mol}^{-1}.$$

The preliminary studies showed that the reaction rate (forward and backward reactions) is sufficient to be used for a TES application [3,4]. This reaction couple is proposed for chemical heat pump application to store and convert heat at temperatures of 370–440 K [32].

Ervin [3] made a cycling study over 500 cycles. He observed a conversion decrease from 95% to 60% within the fortieth cycle. It then stabilized for the next 460 cycles.

Table 3
Advantages and drawbacks of the $CaO/CaCO_3$ system.

Reaction	Advantages	Drawbacks
$CaCO_3 + \Delta H_r \Leftrightarrow CaO + CO_2$	• No catalyst ++ • Industrial technology known for the limestone production + • Material energy density (Theoretical: 692 KWh m^{-3}) +++ • No by-product ++ • Easy product separation (gas-solid) ++ • Availability and price of the product +++	• Agglomeration and sintering − − • Poor reactivity − − − • Change of volume (105%) − • CO_2 storage − • Doping with Ti − −

Table 4
Advantages and drawbacks of the $PbO/PbCO_3$ system.

Reaction	Advantages	Drawbacks
$PbCO_3 + \Delta H_r \Leftrightarrow PbO + CO_2$	• No catalyst ++ • Material energy density (Theoretical: 300 KWh m^{-3}) +++ • No by-product ++ • Product separation (gas-solid) ++	• Poor reversibility − − − • Few experiment feedback − • CO_2 storage − • Toxicity of the products −

The following studies have been done in a Japanese laboratory of the institute of Tokyo, the nuclear reactors laboratory. These researches aimed at developing chemical heat pumps. The first kinetic study of the hydration reaction was led by Kato et al. [33] for 10 μm particles. A 4 steps mechanism between $MgO_{(s)}$ and $H_2O_{(g)}$ has been proposed: (i) containment of water as fixed structural, (ii) physical adsorption of water, (iii) chemical reaction with water producing $Mg(OH)_{2(s)}$ and (iv) inert portion of water. The kinetic parameters have been assessed and the model shows a good accuracy with the experimental results.

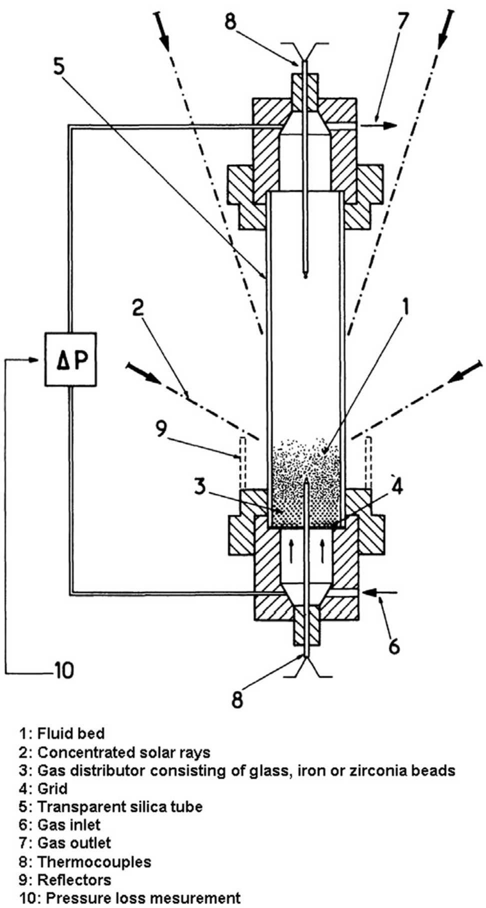


Fig. 7. Solar fluidized bed reactor [19].

Kato et al. [13] led a reversibility study in a thermobalance with a 10 nm $Mg(OH)_2$ powder [32]. In order to get a durable reversibility of the reaction, the authors concluded that the system temperature had to be between 363 and 383 K and the water partial pressure between 47.4 and 57.8 kPa. They observed a constant reversibility with a conversion rate of 50%.

Kato et al. [34,35] have also developed a packed bed reactor used as a chemical heat pump (Fig. 10).

The packed bed (1.8 kg $Mg(OH)_2$) was suspended to a balance in order to measure the mass change of the bed during the reaction. An evaporator and a vacuum pump controlled the water partial pressure in the system. A heating tube controlled the temperature in the system. The operating conditions of dehydration reaction were a temperature of 703 K and a water partial pressure of 14.7 kPa. Regarding the hydration reaction, several water pressures were tested: 31.2, 47.4 and 70.1 kPa. The results showed the possibility to use the chemical heat pump to produce heat at 383 K.

In 2005, Kato et al. [36] developed a new heat pump which is able to operate with partial steam pressure from 30 to 203 kPa. Higher pressures increase the return temperature during the hydration reaction. Here, 52 kg of $Mg(OH)_2$ are introduced in

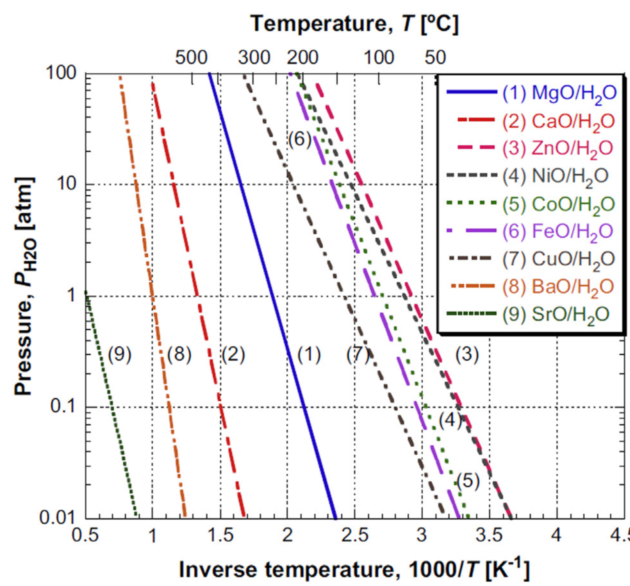


Fig. 9. Equilibrium relationship for metal oxide/water reactions systems [26].

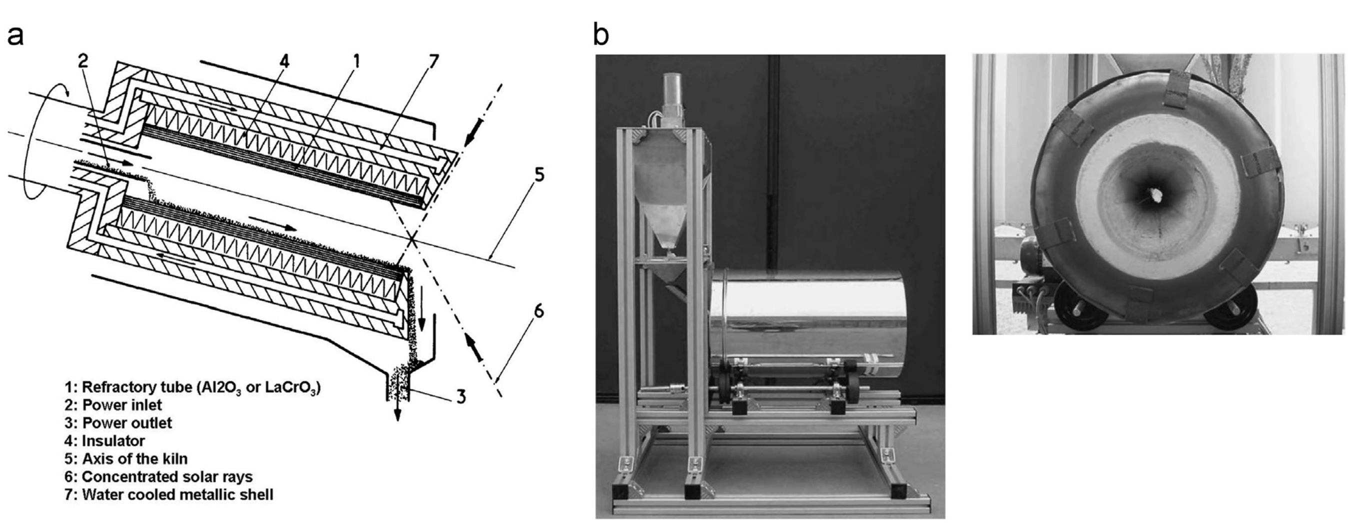


Fig. 8. Solar rotary kiln (a) [19] and (b) [21].

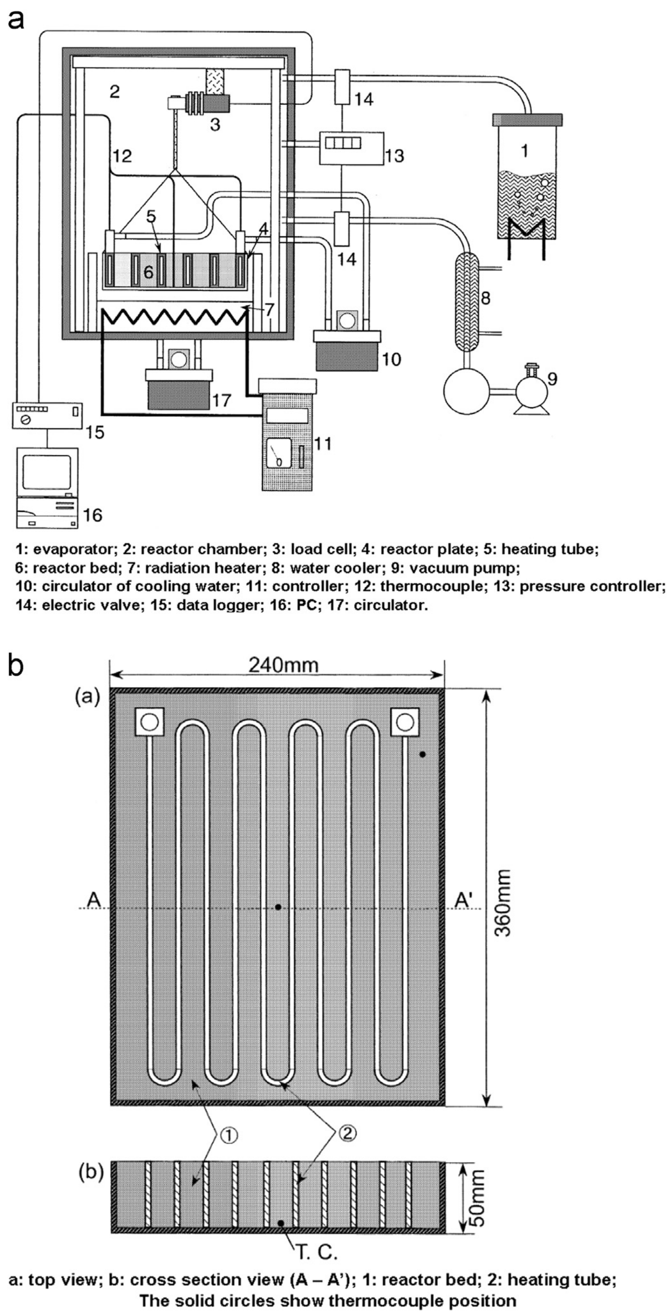


Fig. 10. (a) Laboratory-scale chemical heat pump; (b) reactor bed design [30].

the reactor which is heated by an electrical resistor during the dehydration reaction. For the hydration reaction, the study of the influence of steam partial pressure underlines that for a steam pressure of 203 kPa, the temperatures in the reactor were close to 473 K. Later, the works [31,37–39] dealt with the shaping and the doping of the material in order to diminish the costs and the minimum temperature for dehydration. To reduce the price of $Mg(OH)_2$, the authors used magnesium hydroxide of sea water which they have purified and obtained a cost divided by 10. Concerning the doping, the authors used Ni and LiCl and a decrease of the dehydration temperature of $Mg(OH)_2$ (around 100 K) was observed.

Table 5 presents the advantages and the drawbacks of the $MgO/Mg(OH)_2$ system as thermochemical TES system.

3.4.2. Hydration/dehydration of calcium oxide

The reaction is [40]:

$$Ca(OH)_{2(s)} + \Delta H_r \Leftrightarrow CaO_{(s)} + H_2O_{(g)} \quad \text{with } \Delta H_r = 104 \text{ kJ mol}^{-1}$$

The operating temperatures range from 623 to 1173 K with steam partial pressures from 0 to 2 bar. Many authors studied this reaction for many applications: heat pump, heat storage of concentrated solar plants, motors preheating or electrical generation on the moon. In the following sub-sections, these works are classified into two categories: the heat pumps and the thermal energy storage.

3.4.2.1. The heat pumps. Matsuda et al. [41] studied the kinetics of both the $Ca(OH)_2$ dehydration and the CaO hydration in a thermogravimetric apparatus for heat pump applications. The study have been done with 5 μm $Ca(OH)_2$ particles and 10 mg of product. The following table lists the range of temperature and steam partial pressure for both hydration and dehydration reactions. Table 6

From the end of the 90s to the beginning of the 2000s, most of the studies have been carried out in a Japanese institute, the Kyushu Institute of Technology (KIT) ([41–47]). These works allowed developing and simulating the chemical heat pumps using the couple $CaO/Ca(OH)_2$. These heat pumps work in closed

Table 6
Range of temperature and steam partial pressure for both hydration and dehydration reactions for the kinetic study of Mastuda et al. [41].

Reaction	Temperatures (K)	Steam concentration (vol%)
Dehydration	693–723	1.5–6%
Hydration	356–611	2.0–15.7%

Table 5
Advantages and drawbacks of the $MgO/Mg(OH)_2$ system.

Reaction	Advantages	Drawbacks
$Mg(OH)_2 + \Delta H_r \Leftrightarrow MgO + H_20$	• No catalyst ++ • Material energy density (Theoretical: 380 KWh m^{-3}) +++ • Operating pressure (1 bar) +++ • Good reversibility of the reaction +++ • No by-product ++ • Product separation (gas-solid) ++ • No toxicity + • Experimental feedback (10 years) + • Availability and price of the product ++	• Change of volume - • No industrial feedback - • Product reactivity (50%) -- • Doping - • Low thermal conductivity -

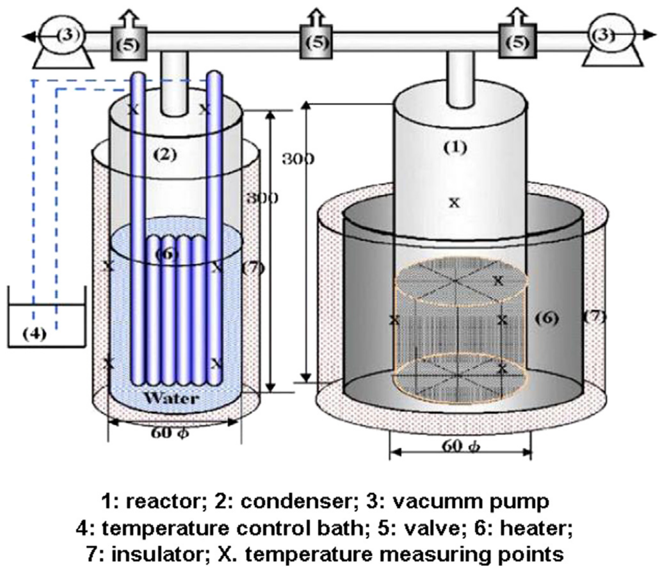


Fig. 11. Standard type chemical heat pump [39].

system and Fig. 11 presents the principle and the operating schemes.

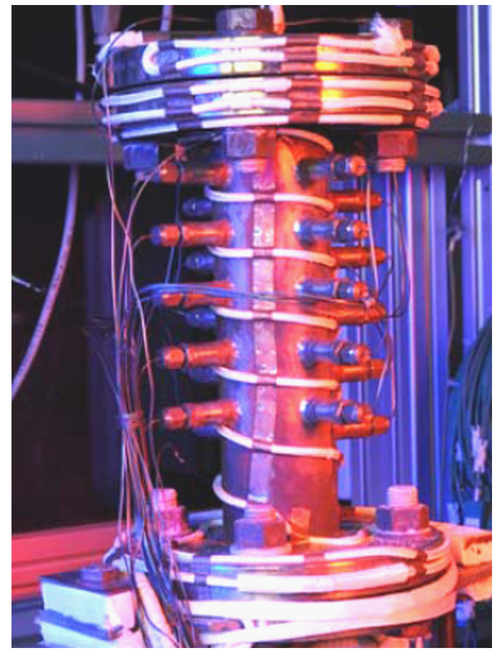


Fig. 12. Experimental setup of a laboratory scale of the DLR system [34].

3.4.2.2. The thermal heat storage. Ervin [3] was the first to suggest using this reaction in a thermal energy storage plant. He achieved 290 cycles with an average conversion rate of 95%. Kanzawa and Arai [48] developed a fixed bed reactor. To increase the heat transfer during the $Ca(OH)_2$ dehydration, they proposed to use a reactor with copper fins. They made a 2D unsteady state model for the fixed bed and determined the optimal distance between the copper fins. Darkwa [49] aimed at developing an energy storage system for the preheating of motors. Experimental and numerical studies have been carried out and he underlined the fact that the heat transfer into the installation limits the reaction. Azpiazu et al. [50] studied the reversibility in a fixed bed reactor with copper fins and 20 cycles were achieved. They observed that using an air atmosphere causes the apparition of a side reaction: the calcium oxide carbonation.

The following studies focus on the development of a thermochemical storage system for applications in solar plants.

Wereko-Brobby [51] worked on the feasibility of the storage system applied to a 1 MWh concentrated solar plant. He suggested using a fluidized bed reactor and he obtained a storage system yield of 45% with reactant storage temperature of 298 K. Brown et al. [52] carried out a technical-economic survey on the development of a thermochemical storage process. The results demonstrate the feasibility of the process for a solar plant with an energy efficiency of 80% and an initial price for the installation of 45 $ kWh_{th}^{-1}. Fujii et al. [53] achieved a study on the kinetics of the particles of calcium hydroxide and calcium oxide as pellets and spheres. The work has been realized with pure products (spheres and pellets) and doped products (pellet) with copper, zinc and aluminum. The best results, for the reaction kinetics are obtained with aluminum doping for an optimal concentration of 15% in weight. Between 2010 and 2013, Schaube et al. [54,55] carried out a survey on the feasibility of the storage process in a thermodynamical solar plant. They used a fixed bed reactor and simulated a one dimensional chemical reactor in unsteady state. They concluded that the heat transfer between the bed and the wall was not a viable solution because the heat conductivity of the material is too low. To improve the heat transfer, they suggested using the circulating gas into the reactor as the heat transfer fluid. In 2012, Schaube et al. [56] worked on the physic-chemical characterization of the products. The authors determined the particles diameter, the specific heat, the reaction enthalpy and the kinetics of both hydration and dehydration with a thermogravimetric analysis. They achieved 100 cycles without reversibility loss. Later, Schaube et al. [57,58] led experimental and numerical studies on the technology of the fixed bed reactor. They used the reactor presented on Fig. 12 for the experimental part and achieved 25 cycles without reversibility loss. The numerical model in two dimensions and in unsteady state has been developed with the COMSOL software. The authors obtained a good accuracy between the simulated and the experimental results.

Table 7 presents the advantages and the drawbacks of the $CaO/Ca(OH)_2$ system as a thermochemical TES system.

3.5. The REDOX system

The general reaction form is

$$M_xO_{y(s)} + \Delta H_r \Leftrightarrow xM_{(s)} + y/2O_2$$

These reactions occur at temperatures between 623 and 1373 K. Only few studies have been made on these materials. The first studied couple was BaO_2/BaO in 1978 [59] and after 30 years without survey, DLR is interested again in these systems for storage application in tower centrals.

3.5.1. Oxidation/decomposition of barium peroxide

The reaction is

$$2BaO_{2(s)} + \Delta H_r \Leftrightarrow 2BaO_{(s)} + O_{2(g)} \quad \text{with } \Delta H_r = 77\ \text{kJ mol}^{-1}.$$

This reaction occurs at temperatures between 673 and 1300 K for partial oxygen pressure between 0 and 10 bar. Preliminary thermogravimetric studies showed the potential of BaO/BaO_2 system for a thermochemical TES application [59,60]. Some difficulties arose when trying to achieve the complete conversion of reaction, because of mass transfer limitations and a crusting of the material surface [60]. The kinetic equations of both forward and reverse reactions were determined and the reaction reversibility had shown a decrease after the first cycle [59]. Recently, Wong et al. [60] studied this couple and compared it with other redox couples for a feasibility study in tower centrals

Table 7
Advantages and drawbacks of the $CaO/Ca(OH)_2$ system.

Reaction	Advantages	Drawbacks
$Ca(OH)_2 + \Delta H_r \Leftrightarrow CaO + H_20$	• No catalyst ++ • Material energy density (Experimental: 300 KWh m^{-3}) +++ • Reversibility of the reaction (~100 cycles) ++ • No by-product ++ • Product separation (gas-solid) ++ • Operating pressure (1 bar) +++ • Availability and price of the product ++ • Nontoxic product + • Experimental feedback (10 years) +	• Agglomeration and sintering −− • Change of volume (95%) − • Low conductivity −

Table 8
Advantages and drawbacks of the BaO/BaO_2 system.

Reaction	Advantages	Drawbacks
$2BaO_2 + \Delta H_r \Leftrightarrow 2BaO + O_2$	• Operating temperature (400–1300 K) ++ • O_2 reactant ++ • No catalyst ++ • No side reaction ++ • Products separation (gas-solid) ++ • Operating pressure (0–10 bar) ++	• Incomplete conversion of both forward and reverse reactions −−− • No experiment feedback −

Table 9
Advantages and drawbacks of the Co_3O_4/CoO system.

Reaction	Advantages	Drawbacks
$2Co_3O_4 + \Delta H_r \Leftrightarrow 6CoO + O_2$	• High reaction enthalpy (~205 kJ mol^{-1}) ++ • O_2 as a reactant ++ • No catalyst ++ • No by product ++ • Reversibility (500 cycles) +++ • Products separation (gas-solid) ++	• Few experiment feedback − • Storage of O_2 −− • Toxicity of the products − • Cost of the products −−−

Table 10
Advantages and drawbacks of the $NH_4HSO_4/NH_3/H_2O/SO_3$ system.

Reaction	Advantages	Drawbacks
$NH_4HSO_4 + \Delta Hr \Leftrightarrow NH_3 + H_2O + SO_3$	• Material energy density (Theoretical: 860 KWh m^{-3}) +++ • No catalyst ++ • Product separation (gas-liquid) ++	• Corrosive products −−− • Toxic products − • No experiment feedback −

Table 8 presents the advantages and the drawbacks of the BaO/BaO_2 system as thermochemical TES system.

3.5.2. *Other oxidation/decomposition peroxide couples*

More recently, a study about the potential of six oxide/peroxide couples for a thermochemical TES application has been investigated by Wong et al. [61]. To assess the relevance of various couples, a thermodynamic analysis, an engineering feasibility study and thermogravimetric measurements have been done. The relevant couples are: Co_3O_4/CoO, MnO_2/Mn_2O_3, CuO/Cu_2O, Fe_2O_3/FeO, Mn_3O_4/MnO and V_2O_5/VO_2. Nevertheless, for their application, the most promising reaction is:

$$2Co_3O_{4(s)} + \Delta H_r \Leftrightarrow 6CoO_{(s)} + O_{2(g)} \quad \text{with } \Delta H_r = 205 \text{ kJ mol}^{-1}.$$

The decomposition occurs at 1123 K in a nitrogen atmosphere and the oxidation occurs at 973 K in an air atmosphere with partial oxygen pressure between 0 and 1 bar. This reaction has been implemented both in a thermogravimetric balance and in a fixed bed [62]. 500 cycles have been achieved and the morphologic study of the product showed a progressive magnification of the particles progressively during the cycles. Buckingham et al. [63] have done a numerical analysis of packed bed parameters and operating conditions. They

concluded that a packed bed design for metal oxide TES couple will not be economically competitive and recommended to study a “moving bed” design, as a rotary kiln, to improve the TES process.

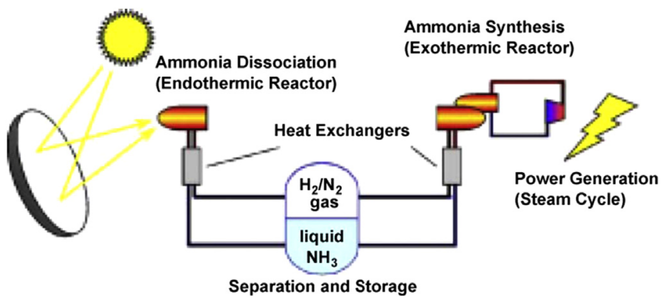


Fig. 13. Installation of a parabolic through power plant with chemical energy storage [49].

Neises et al. [64] used a rotary kiln based on the work of Buckingham et al. [63] to implement the reaction which is heated through a solar furnace of 22 kW. They carried out a reversibility study on three samples: pure Co_3O_4 and two mixtures of doped Co_3O_4 with alumina oxide. They achieved 30 cycles and demonstrated the feasibility of the process with an energetic density in the reactor of 95 kWh m^{-3}.

Table 9 presents the advantages and the drawbacks of the Co_3O_4/CoO system as the thermochemical TES system.

3.6. Ammonia system

Historically, two reactions using the “Ammonia system” have been studied. The first one, studied by Wenthworth et Chen [5] is the decomposition of NH_4HSO_4 but only few surveys have been carried out. The second one, studied by the Australian National University (ANU) since 40 years, is the decomposition/synthesis of the ammonia for thermal energy storage.

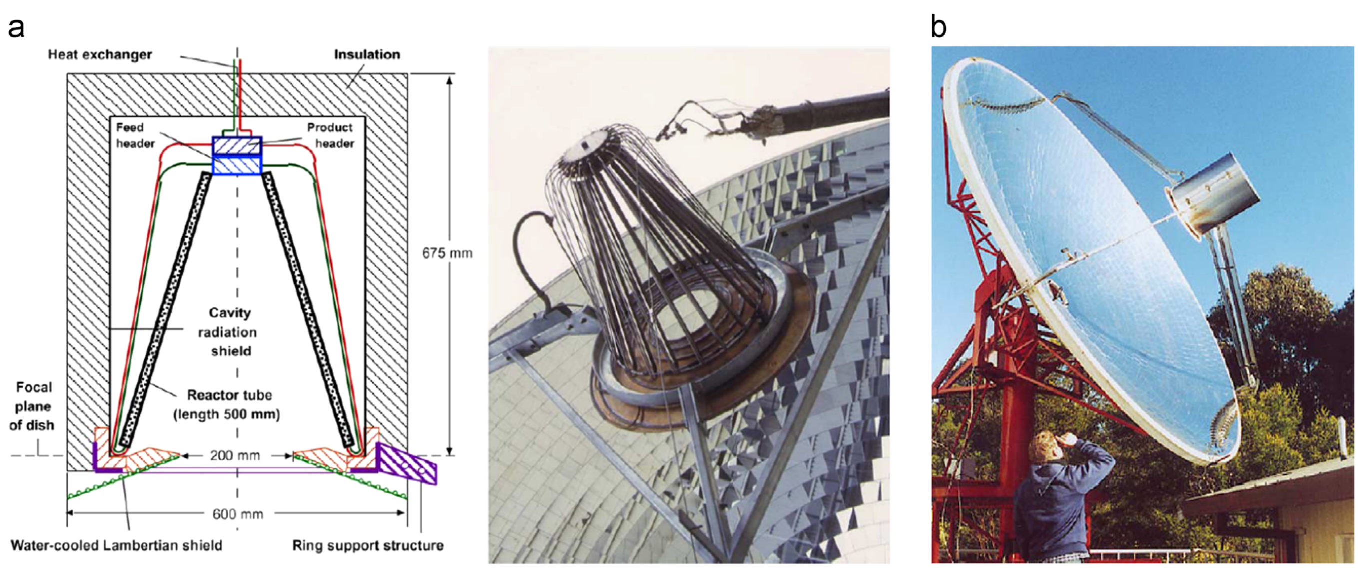


Fig. 14. Solar ammonia dissociation reactor (a) design of the cavity receiver with 15 kW_{sol} and its assembly on ANU's 20 m^2 dish without insulation fitted; and (b) reactor in operation on the ANU's 20 m^2 dish [49].

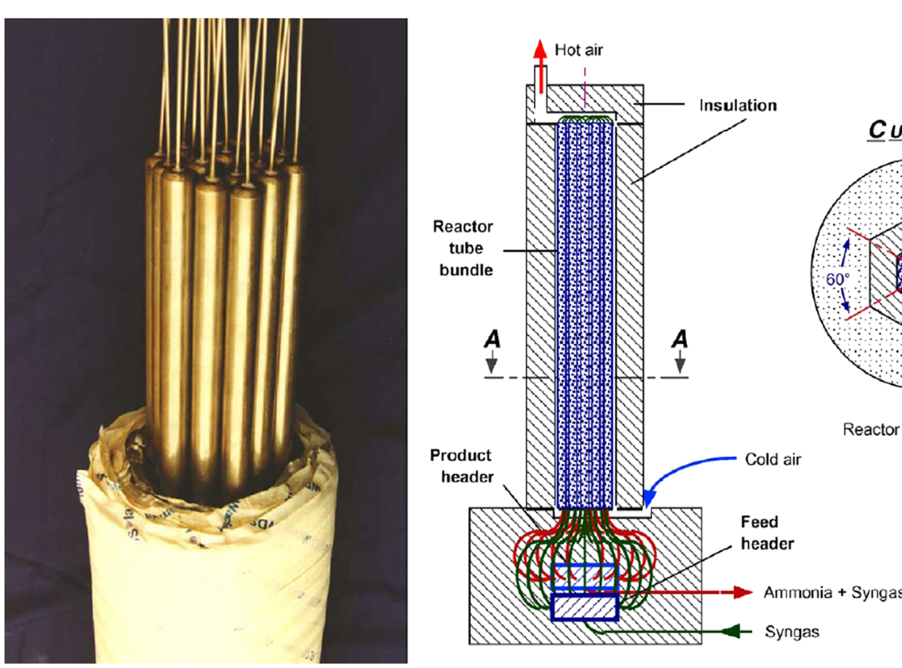


Fig. 15. Design of the 10 kW_{th} ammonia synthesis heat recovery [49].

3.6.1. *The ammonium hydrogen sulfate system*

The reaction is

$$NH_4HSO_{4(l)} + \Delta H_r \Leftrightarrow NH_{3(g)} + H_2O_{(g)} + SO_{3(g)} \quad \text{with } \Delta H_r = 336 \text{ kJ mol}^{-1}.$$

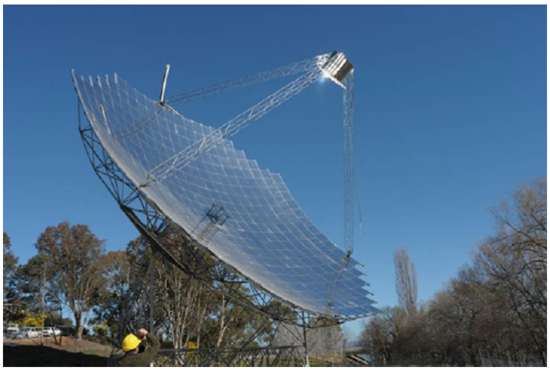


Fig. 16. ANU's 500 m^2 paraboloidal dish concentrator [57].

A preliminary study showed the potential of this system for TES application [5]. The reaction occurs at 690 K and 1.46 atm. No catalysts are required for both forward and reverse reactions. A process flowsheet was designed to carry out a thermochemical TES process based on ammonium hydrogen sulfur cycle [5]. Prengle et al. [5] defined the thermal efficiency as the ratio between the released heat energy and the required solar energy. The preliminary energy analysis of the cycle confirmed the engineering feasibility of the process with a thermal efficiency of 62% and a theoretical energetic density of 860 kWh m^{-3}.

Table 10 presents the advantages and the drawbacks of the $NH_4HSO_4/NH_3/H_2O/SO_3$ system as the thermochemical TES system.

3.6.2. *Dissociation/synthesis of NH_3*

The reaction is

$$2NH_{3(g)} + \Delta H_r \Leftrightarrow N_{2(g)} + 3H_{2(g)} \quad \text{with } \Delta H_r = 66.9 \text{ kJ mol}^{-1}.$$

This reaction occurs at temperatures between 673 and 973 K and pressures between 10 and 30 bar. The Haber–Bosch process is based on this reaction for the NH_3 production since 100 years. A lot of

Table 11
Advantages and drawbacks of the $NH_3/N_2/H_2$ system.

Reaction	Advantages	Drawbacks
$2NH_{3(g)} + \Delta H_r \Leftrightarrow N_{2(g)} + 3H_{2(g)}$	• Ammoniac synthesis known since 100 years (Haber-Bosch process) ++ • Ammoniac: liquid at ambient conditions ++ • ANU's important experiment feedback (40 years) + • No side reaction ++	• H_2 and N_2 storage (gases) - • Use of catalyst (Fe/Co) -- • Operating pressure (80–200 bar) --- • Incomplete conversion of both forward and reverse reactions ---

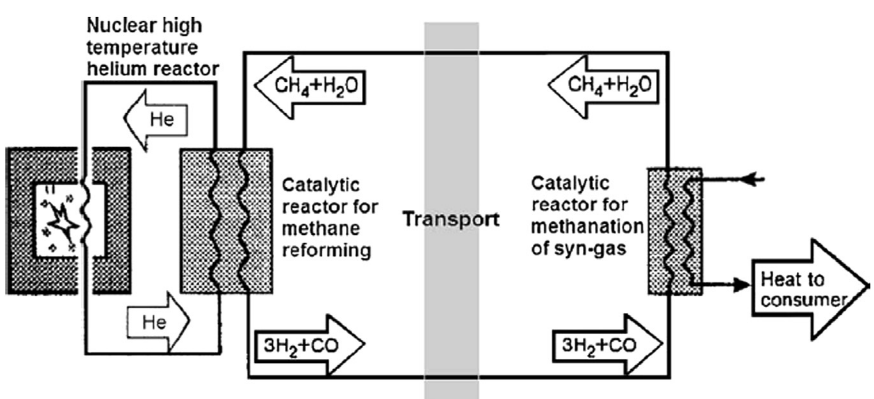


Fig. 17. Schematic diagram of the EVA-ADAM process cycle for heat conversion and transportation of nuclear energy [58].

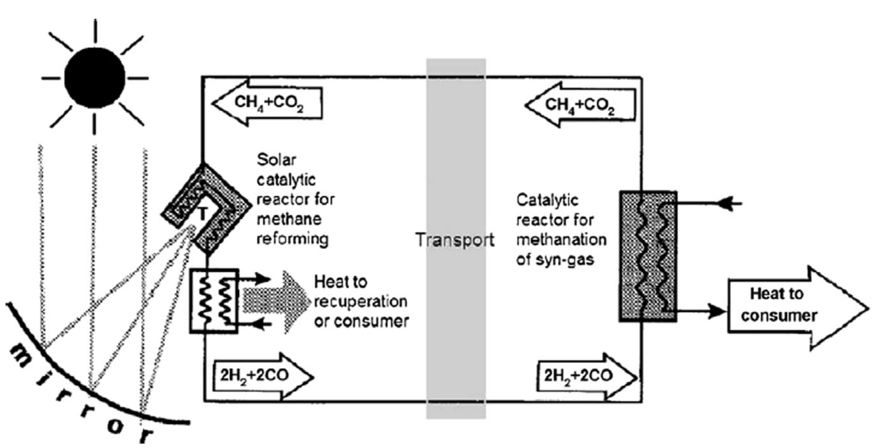


Fig. 18. Schematic diagram of reforming methane process cycle using carbon dioxide for heat conversion and transportation of concentrated solar energy [58].

studies (e.g.: kinetic studies by Temkin et al. [65]) have already been done for this application (NH_3 production). Fig. 13 shows the scheme of the installation developed and used by the Australian National University (ANU) for a thermochemical TES application.

Both forward and reverse reactions are catalysed. The catalyst materials used in the endothermic reactor and in the exothermic reactor are respectively the Haldor-TopsØe "DNK-2R" [66] and Haldor-TopsØe "KM1" [67].

The works on a thermochemical TES system using the ammonia system began with Carden [68] and Williams and Carden [69]. They assessed a theoretical energetic efficiency of 90% if the conversion rate of the ammonia into the reactor was higher than 60%. Later, the thermodynamic limitations associated with the use of the reversible reaction of the ammonia have been studied by Lovegrove et al. [70,71] thanks to a pseudo-homogeneous two dimensions model of reactor. The first solar driven high pressure ammonia reactor of 1 kW has been successfully tested in a closed loop system [67]. This reactor allowed the validation of a numerical model to predict the temperatures in the catalyst, on the wall and in the gas, and also the conversion rate and the product flowrates. A detailed study of a 10 MW_e base load power plant in Australia, has indicated that levelled electricity costs lower than AUS $ 0.15/kWh were potentially achievable [72]. A scale-up (Fig. 14) of the first solar driven ammonia reactor has been done in order to accept the full (=15 kW) input from the ANU's 20 m^2 dish system [66].

Fig. 15 shows the design of the ammonia synthesis heat recovery reactor of 10 kW_{th} [66].

A new 500 m^2 parabolic dish solar concentrator has been built by the ANU in 2009 (Fig. 16). The receiver geometry was numerically optimized to improve the dissociation reaction [73]. This numerical model can then be applied to develop an ammonia receiver for the 500 m^2 SG4 dish concentrator.

ANU has done the most advanced works in this sector, by working for over 40 years on the thermochemical energy storage using the dissociation and synthesis of ammonia. ANU is also the first laboratory which continuously store and release energy during 24 h thanks to its closed loop system composed of a solar reactor of 15 kW for the dissociation reaction and a synthesis reactor of 10 kW [75].

Table 11 presents the advantages and the drawbacks of the $NH_3/N_2/H_2$ system as the thermochemical TES system.

3.7. *Organic systems*

3.7.1. *Methane reforming*

Reforming of methane using steam or carbon dioxide is industrially used for the H_2 production. These reactions have also been studied for heat transportation. There is no study about the TES system based on the methane reforming, but this could be an application. Both reactions are catalysed by Ni-based or Ru-based catalysts [76].

3.7.1.1. Methane steam reforming. The reaction is

$$CH_{4(g)} + H_2O_{(l)} + \Delta H_r \Leftrightarrow CO_{(g)} + 3H_{2(g)} \quad \text{with } \Delta H_r = 250 \text{ kJ mol}^{-1}{}_{CH_4}.$$

The side reaction is

$$CO_{(g)} + H_2O_{(l)} \Leftrightarrow CO_{2(g)} + H_{2(g)} + \Delta H_r \quad \text{with } \Delta H_r = -41.2 \text{kJ mol}^{-1}{}_{CO}.$$

This reaction occurs at temperatures between 873 and 1223 K and pressures between 20 and 150 bar. In 1975, Kugelers et al. [77] suggested to use the reaction of methane steam reforming for the transport of the thermal energy coming from the nuclear plants. The authors made a feasibility survey and proposed a process flowsheet (Fig. 17) with energetic efficiencies between 60% and 73%. In order to study and understand the phenomena involved during the reaction, a first pilot plant, EVA I, was built by Fedders et al. [78]. An industrial-scale pilot plant EVA I/ADAM I of 300 kW was developed in 1979 at the Intitut für Reaktorbauelemente in Germany. 850 operating hours have been investigated. They showed the feasibility of the energy transport system by means of the reversible reaction [79]. More recently, a new design process (ICAR: immediate catalytic accumulation of ionizing radiation energy) was developed by Aristov et al [80]. The endothermic reactor is directly combined with the nuclear reactor to improve the process efficiency.

3.7.1.2. Methane reforming using carbon dioxide. Methane reforming using carbon dioxide presents an advantage for a TES

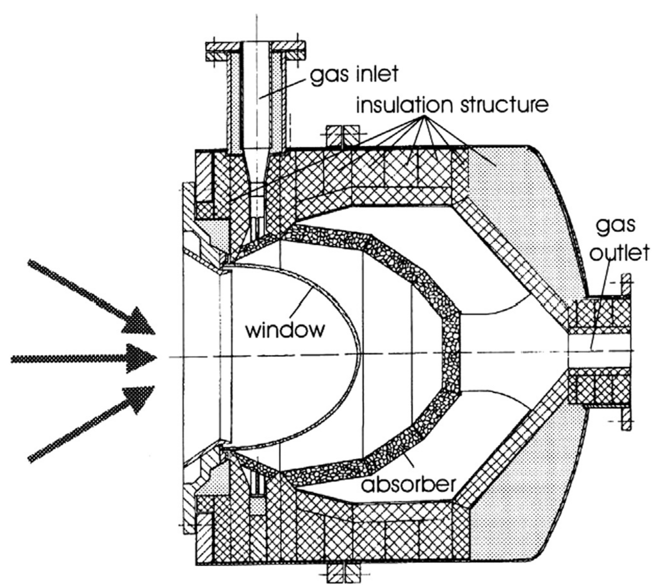


Fig. 19. Schematic of the solar chemical receiver–reactor [64].

Table 12
Advantages and drawbacks of the CH_4/CO_2 and the CH_4/H_2O systems.

Reaction	Advantages	Drawbacks
$CH_4+H_2O+\Delta H_r \Leftrightarrow 3H_2+CO$	• Industrial feedback + • High reaction enthalpy (~250 kJ mol^{-1}) ++ • Gas phase +	• H_2 storage − • Cost of CH_4 −− • Side reactions −−− • Use of catalyst −− • Low reversibility −−
$CH_4+CO_2+\Delta H_r \Leftrightarrow 2H_2+2CO$		

Table 13
Advantages and drawbacks of the C_6H_{12}/C_6H_6 system.

Reaction	Advantages	Drawbacks
$C_6H_{12}+\Delta H_r \Leftrightarrow C_6H_6+3H_2$	• Industrial feedback + • Operating temperature (~580 K) +++	• H_2 storage - • Use of Catalyst -- • Secondary reaction -- • Toxic products - • Reversibility ---

Table 14
Advantages and drawbacks of the $SO_3/SO_2/O_2$ system.

Reaction	Advantages	Drawbacks
$2SO_3+\Delta H_r \Leftrightarrow 2SO_2+O_2$	• Industrial feedback with the H_2SO_4 production + • Operating temperature (773–1223 K) +++ • O_2 as a reactant +	• Corrosive product --- • Toxic product - • Need of catalyst -- • Storage of H_2 -

application compared to the steam reforming process. It does not involve water evaporation [76].

The carried out reaction is

$$CH_{4(g)}+CO_{2(g)}+\Delta H_r \Leftrightarrow 2CO_{(g)}+2H_{2(g)} \quad \text{with } \Delta H_r = 247 \text{ kJ mol}^{-1}{}_{CH^4}.$$

The side reaction is:

$$CO_{2(g)}+H_{2(g)}+\Delta H_r \Leftrightarrow CO_{(g)}+H_2O_{(g)} \quad \text{with } \Delta H_r = -41.2 \text{ kJ mol}_{CO}{}^{-1}.$$

Fig. 18 shows the process flowsheet. During the endothermic reaction, methane and carbon dioxide are decomposed at a temperature between 973 and 1133 K and absolute pressure of 3.5 bar to form hydrogen and carbon monoxide. Edwards and Maitra [81] outlined the potential of this reforming for TES application. Edwards et al. [82] achieved a technical-economic survey in order to evaluate the energetic efficiencies of two different processes for a production of 100 MWe. The first one works in closed loop (Solar/Rankine cycle plant) and the second one in open loop (Solar/Gas turbine combined cycle). Both cases have energetic efficiencies of 33.6% and 44.6%.

Later, the DLR [83] developed a solar reactor of 300 kW to implement the reforming reaction (Fig. 19). This solar reactor has been used in a global test loop at the WIS (Weizmann Institute of Science) in Rehovot, Israel. Nevertheless, in spite of good conversion rate of methane, many problems of catalyst deactivation appeared due to a deposit of sodium.

Table 12 presents the advantages and the drawbacks of the CH_4/CO_2 and the CH_4/H_2O systems as thermochemical TES system.

3.7.2. *Cyclohexane dehydrogenation – benzene hydrogenation*

The carried out reaction is

$$C_6H_{12(g)}+\Delta H_r \Leftrightarrow C_6H_{6(g)}+3H_{2(g)} \quad \text{with } \Delta H_r = 206 \text{ kJ mol}^{-1}.$$

This reaction is well known in the chemical industry and the reactor technologies to carry out both forward and reverse reactions are known. During the charging step, the cyclohexane is heated up to 566 K at 1 bar at which the endothermic reaction occurs. The decomposition reaction products are hydrogen (gas) and benzene (gas). During the storing step, benzene can be stored as a liquid at atmospheric pressure and hydrogen has to be compressed and stored. During the discharging step, benzene and hydrogen are mixed at 610 K and 70 bar to generate heat and the initial cyclohexane. Both forward and reverse reactions are catalysed [4]. Process simulations of chemical heat pumps were investigated to improve the coefficient of performance (COP) [80,84].

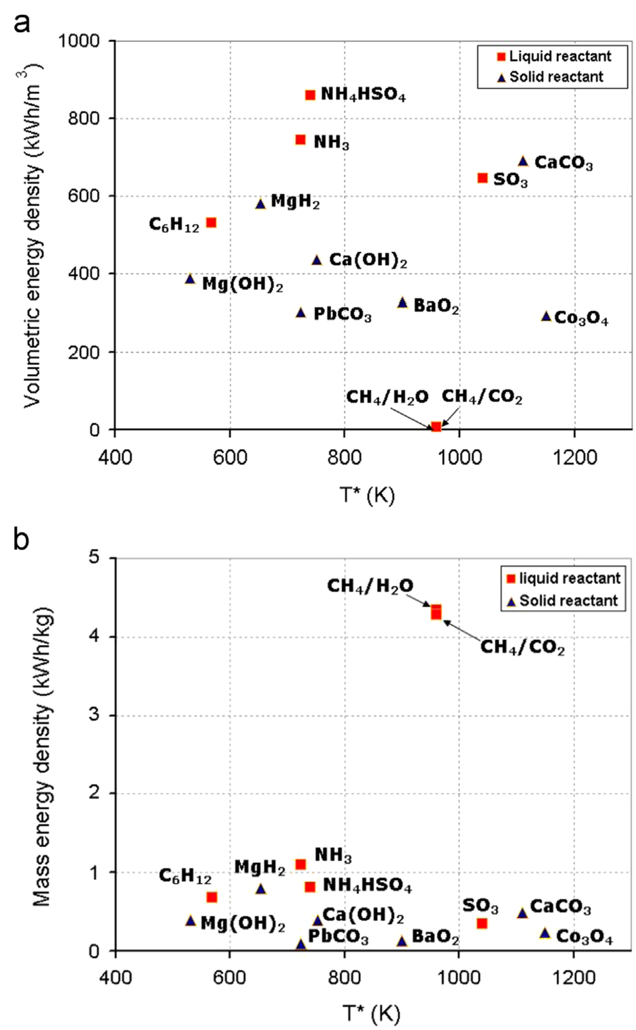


Fig. 20. Energy density versus turning temperature for the reversible reactions studied as a TES system in the literature: (a) volumetric energy density; and (b) mass energy density.

Table 13 presents the advantages and the drawbacks of the C_6H_{12}/C_6H_6 system as the thermochemical TES system.

Table 15
Literature data about reversible reactions studied for thermochemical storage systems (temperature range of 573–1273 K).

Reaction	Phase	Reaction enthalpy (kJ/ mol_A)	Operating temperature conditions	Energetic density	Related works	Technology	References
Hydride system							
$MgH_2 + \Delta H_r \Leftrightarrow Mg + H_2$	Solid-gas	ΔHr = 75 kJ/mol	Heat Charge: 653 K Heat release: 503 K	– 580 kWh/m^3_{MgH2} – 0.80 kWh/kg_{MgH2}	– Kinetic study – Reversibility study – Reactor design – heat exchanger design – Review	– Steam generator (3.6 kWh) – Packed bed reactor – Solar power station – Solar cooking and cooling device – Heat exchanger	[17,18]
Carbonate system							
$PbCO_3 + \Delta H_r \Leftrightarrow PbO + CO_2$	Solid-gas	ΔHr = 88 kJ/mol	– Heat charge: 723 K – Heat Release: 573 K	– 303 kWh/m^3_{PbCO3} – 0.09 kWh/kg	– Equilibrium relationship – Kinetics study	– TGA (thermogravimetric analysis)	[28–30]
$CaCO_3 + \Delta H_r \Leftrightarrow CaO + CO_2$	Solid-gas	ΔHr = 178 kJ/mol	– Heat charge: 1133 K – Heat release: 1153	– 692 kWh/m^3_{CaCO3} – 0.49 kWh/kg $_{CaCO3}$	– Reversibility – Reactivity – Reactor design – Decarbonation reactor – CO_2 capture – Review	– TGA – Fluidised bed reactor – Packed bed reactor – Chemical heat pump – Horizontal rotary reactor	[13,19–27]
Hydroxide system							
$Mg(OH)_2 + \Delta H_r \Leftrightarrow MgO + H_2O$	Solid-gas	ΔHr = 81 kJ/mol	– Heat charge: 423 K – Heat release: 373 K	– 388 kWh/$m^3_{Mg(OH)2}$ – 0.39 kWh/$kg_{Mg(OH)2}$	– Equilibrium relationship – Kinetic study – Reversibility – Reactor design	– TGA – Packed bed reactor – Chemical heat pump	[3,4,31–36]
$Ca(OH)_2 + \Delta H_r \Leftrightarrow CaO + H_2O$	Solid-gas	ΔHr = 104 kJ/mol	– Heat charge: 723 K – Heat release: 298–673 K	– 437 kWh/$m^3_{Ca(OH)2}$ – 0.39 kWh/kg $_{Ca(OH)2}$	– Equilibrium relationship – Kinetic study – Reversibility – Reactor design – Simulation – Heat transfer enhancement – Cost analysis	– TGA – Packed bed reactor – Chemical heat pump	[3,4,40–58]
Ammonium system							
$NH_4HSO_4 + \Delta H_r \Leftrightarrow NH_3 + H_2O + SO_3$	Liquid-gas	ΔHr = 336 kJ/mol	– Heat charge: 1200 K – Heat release: 700 K	– 860 kWh/ $m^3_{NH4HSO4}$ – 0.81 kWh/ $kg_{NH4HSO4}$	– Theoretical analysis – Thermodynamics analysis – Process simulation	[–]	[4,5]
$2NH_{3(g)} + \Delta H_r \Leftrightarrow N_{2(g)} + 2H_{2(g)}$	Gas	ΔHr $_{Heat\ Charge}$ = 66.9 kJ/ mol ΔHr $_{Heat\ Release}$ = 53 kJ/mol	Heat charge: 723 K; P = 9–150 bar Heat release: 723 K; P = 10–300 bar	745 kWh/$m^3_{NH3(l)}$ 1.09 kWh/$kg_{NH3(l)}$	– Kinetic study – Process simulation – Technical and economical feasibility study – Reactor design study – Ammonia receiver design	– 1 $kW_{chem.}$ Laboratory-scale ammonia dissociation and synthesis reactor – 10 $kW_{chem.}$ Laboratory-scale ammonia dissociation and synthesis reactor – Ammonia receiver design for a 500 m² dish	[4,65–74,87–89]

REDOX system							
$2Co_3O_4 + \Delta H_r \Leftrightarrow 6CoO + O_2$	Solid-gas	ΔHr = 205 kJ/mol	T = 1143–1173 K	– 295 kWh/m^3_{Co3O4} – 0.24 kWh/kg $_{Co3O4}$	– Equilibrium analysis – Kinetic study – Mixed oxide reaction – Thermodynamic analysis	– TGA – Packed bed reactor	[61,63]
$2BaO_2 + \Delta H_r \Leftrightarrow 2BaO + O_2$	Solid-gas	ΔHr = 77 kJ/mol	T = 963–1053 K	– 328 kWh/m^3_{BaO2} – 0.13 kWh/kg_{BaO2}	– Equilibrium analysis – Kinetic study	– TGA	[59,60]
Organic system							
$CH_4 + H_2O + \Delta H_r \Leftrightarrow 3H_2 + CO$	Gas	250 kJ/mol	– Heat charge: 1223 K – Heat release: 803 K	– 7.8 kWh/$m^3_{CH4(g)}$ – 4.34 kg/$kg_{CH4(g)}$	– Process simulation – Reactor design – Kinetic study – Energy transport	– Laboratory pilot plant – Industrial size pilot plant 300 $kW_{transported}$(EVA I/ADAM I)	[76–80]
$CH_4 + CO_2 + \Delta H_r \Leftrightarrow 2H_2 + 2CO$	Gas	247 kJ/mol	– Heat charge: 1223 K – Heat release: 803 K	– 7.7 kWh/$m^3_{CH4(g)}$ – 4.28 kg/$kg_{CH4(g)}$	– Technical and economical feasibility study – Reactor design – Energy transport	– Design of the receiver reactor 200–300 kW (DLR)	[76,79,81–83]
$C_6H_{12} + \Delta H_r \Leftrightarrow C_6H_6 + 3H_2$	Liquid-gas	ΔHr = 206.7 kJ/mol	Heat charge: T = 590 K Heat release: T = 670 K	530 kWh/$m^3_{C6H12(l)}$ 0.68 kWh/$kg_{C6H12(l)}$	– Process simulation analysis in chemical heat pump	[–]	[4,80,84]
SO_3 system							
$2SO_3 + \Delta H_r \Leftrightarrow 2SO_2 + O_2$	Liquid-Gas	ΔHr = 98 kJ/mol	Heat charge: 1073–1273 K Heat release: 773–873 K	646 kWh/$m^3_{SO3(l)}$ 0.34 kWh/$kg_{SO3(l)}$	– Process analysis to produce a continuous 100 MW electric power output	[–]	[4,85]

3.7.3. Thermal dissociation of sulfur trioxide

The reaction is

$$2SO_{3(g)} + \Delta H_r \Leftrightarrow 2SO_{2(g)} + O_{2(g)} \quad \text{with } \Delta H_r = 98 \text{ kJ mol}^{-1}_{SO_{3(G)}}.$$

This reaction occurs at temperatures between 773 and 1373 K for pressures between 0.1 and 0.5 MPa. During the charging step, the liquid sulfur trioxide is heated up to vaporization. This phase change requires 43 kJ $mol^{-1}_{SO_{3(l)}}$. The gas product is heated up to the decomposition temperature (1073–1373 K), at which the endothermic reaction occurs. The endothermic reaction has to be catalysed, generally with V_2O_5 [4,85]. The decomposition reaction products are sulfur dioxide (gas) and oxygen (gas). During the discharging step, the oxygen is added to the sulfur dioxide to regenerate the heat (773–973 K) and the initial sulfur trioxide. A process analysis has been done by Chubb [85] to use this reaction in a Solchem system to produce a continuous 24 h electricity output of 100 MW with a 72 h storage. A process simulation assessed the thermal efficiency to 58% [4].

Table 14 presents the advantages and the drawbacks of the $SO_3/SO_2/O_2$ system as the thermochemical TES system.

3.8. Summary of case studies

Several numerical, experimental and technological studies concerning thermochemical energy storage have been found in the literature. Fig. 20a and b plot the volumetric energy density and the gravimetric energy density versus the turning temperature of the studied reactions. To assess the volumetric energy density of the solid reactant, the bulk density with a packed bed porosity of 0.5 has been chosen. Usually, a packed bed porosity of spherical particle is between 0.4 and 0.5 [86]. The volume of pores inside a particle is considered to be equal to zero.

Fig. 20 is extremely useful to quickly screen the candidate reactions in the desired temperature and the energy density ranges. Each reaction system is detailed in Table 15. Table 15 lists the reversible reaction, the phase of the A reactant, the reaction enthalpy by mol of reactant A, the operating temperatures, the energy density and the related works and technologies.

4. Conclusion

This paper presents a state of the art of the current numerical and experimental researches on chemical reactions for high temperature thermochemical heat energy storage. Most of the described systems were only tested on laboratory scale until now. This paper has also offered an updated review of the high temperature (573–1273 K) thermochemical TES system which have the potential to become an important part of sustainable handling of energy in a close future. The following conclusions that can be drawn are

- The energy density of a thermochemical TES system ($\sim$500 kWh m^{-3}) is 5 to 10 times higher than latent heat storage systems and sensible heat storage systems respectively.
- Thermochemical TES systems appear to be the most promising way to store solar thermal energy during a long-term period. Indeed, both storage period and transport distance are theoretically unlimited because there is no loss of thermal energy during storage as products can be stored at ambient temperature.
- Laboratory-scale experiments, numerical and technological studies have demonstrated the feasibility of several reaction systems for a TES application.
- The system involving the ammonia dissociation and synthesis is the most mature technology for a high temperature TES application with 40 years of researches and pilot-scale equipment.
- The dehydration/hydration of the $Ca(OH)_2/CaO$ couple shows a high potential for TES application but future works need to focus on the intensification of heat and mass transfers inside the reactor.
- For a high temperature thermochemical heat storage (CSP application), the following chemical reactions seem to be the most interesting ones in terms of actual development, cost and temperature range:

$$MgH_2 \Leftrightarrow Mg + H_2$$

$$PbCO_3 \Leftrightarrow PbO + CO_2$$

$$Ca(OH)_2 \Leftrightarrow CaO + H_2O$$

$$NH_3 \Leftrightarrow N_2 + H_2$$

Nowadays, the storage system with the reaction couple $NH_3 \Leftrightarrow N_2 + H_2$ is the most mature one especially with the ANU works and their 40 years feedback. Nevertheless, recently the reaction couple $Ca(OH)_2 \Leftrightarrow CaO + H_2O$ appears to be promising for thermochemical heat storage and many studies and projects contribute to develop this system. The main barriers to remove are linked to the reactor heat and mass transfers. As a consequence the development of intensified heat exchanger/reactor could be interesting to study. Mass transfer issues have also to be addressed, especially if fast hydration and dehydration kinetics are expected. A compromise between particle diameter and mass transfer limitation will have to be found and future works could focus on the functionalization of the particles, supported particles or doping. Moreover, for G/S reactions in general, an effort should be done on the optimization of the particle size and the reaction bed structure to guarantee a constant heat output during the discharging step. This optimization must be done without compromising, as far as possible, the system compactness.

Another area of research is the optimization of the temperature level during charging/discharging steps. The objective is to diminish the difference of temperature between both steps to improve the efficiency and the ease to control the process and the downstream turbine for instance.

At present, only laboratory and pilot experiments have been done and scale-up is an important point to address. Large-scale experiments are necessary to prove the feasibility of the thermochemical TES system for both short and long-term storage. The process must be reversible with a constant conversion rate and without degradation after a large number of cycles. To support the scale-up procedure, numerical models of the storage process have to be developed. The objective is to insert them in the whole power plant scheme to assess the performances according to the application case (seasonal storage, 24 h electricity production, peak load,…).

The future works should also allow the definition of a methodology to choose suitable materials for a given TES application. Technical-economic studies will be required to assess the profitability of the whole TES process. Thus, storage materials, storage equipment, control strategies of the system and applications cases are important points to address.

References

[1] Gil A, Medrano M, Martorell I, Lazaro A, Dolapo P, Zalba B, et al. State of the art on high temperature thermal energy storage for power generation. Part 1 – concepts, materials and modelisation. Renew Sust Energy Rev 2010;14 (1):31–55.

[2] Medrano M, Gil A, Martorell I, Potau X, Cabeza LF. State of the art on high-temperature thermal energy storage for power generation. Part 2 – case studies. Renew Sust Energy Rev 2010;14(1):56–72.

[3] Ervin G. Solar heat storage using chemical reactions. J Solid State Chem 1977;22:51–61.
[4] Garg HP, Mullick SC, Bhargara AK. Solar thermal energy storage. Dordrecht, Holland: D. Reidel Publishing Company; 1985.
[5] Wentworth WE, Chen E. Simple thermal decomposition reactions for storage of solar thermal energy. Sol Energy 1976;18:205–14.
[6] Edem N'Tsoukpoe K, Liu H, Le Pierres N, Luo L. A review on long term sorption solar energy storage. Renew Sust Energy Rev 2009;13:2385–96.
[7] Wongsuwan W, Kumar S, Neveu P, Meunier F. A review of chemical heat pump technology and applications. Appl Therm Eng 2001;21:1489–519.
[8] Cot-Gores J, Castell A, Cabeza LF. Thermochemical energy storage and conversion: A state-of-the-art review of the experimental research under practical conditions. Renew Sust Energy Rev 2012;16:5207–24.
[9] Felderhoff M, Urbanczyk R, Peil S. Thermochemical heat storage for high temperature applications – a review. Green 2013;3:113–23.
[10] Zalba B, Marin JM, Cabeza LF, Mehling H. Review on thermal energy storage with phase change: materials, heat transfer analysis and applications. Appl Therm Eng 2003;23:251–83.
[11] Kenisarin MM. High temperature phase change materials for thermal energy storage. Renew Sust Energy Rev 2010;14:955–70.
[12] Kato Y. Possibility of chemical heat storage in thermal energy transportation market. IEA, ECES IA Annex 18, Transportation of energy utilizing Thermal Energy Storage Technology. In: 1st Workshop, 13–15 November 2006, Tokyo, Japan.
[13] Kyaw K, Matsuda H, Hasatani M. Applicability of carbonation/decarbonation reactions to high-temperature thermal energy storage and temperature upgrading. J Chem Eng Jpn 1996;29(1):119–25.
[14] Harries. DN, Paskevicius M, Sheppard DA, Price TEC, Buckley CE. Concentrating solar thermal heat storage using metal hydrides. Proc IEEE 2012;100(2):539–49.
[15] Yang FS, Wang GX, Zhang ZX, Rudolph V. Investigation on the influences of heat transfer enhancement measures in a thermally driven metal hydride heat pump. Int J Hydrog Energy 2010;35:9725–35.
[16] Paskevicius M, Sheppard DA, Buckley CE. Thermodynamics changes in mechanochemically synthesized magnesium hydride nanoparticles. J Am Chem Soc 2010;132:5077–83.
[17] Bogdanović B, Ritter A, Spielthoff B. Active MgH_2–Mg systems for reversible chemical energy storage. Angew Chem Int Ed Engl 1990;29(3):223–328.
[18] Felderhoff M, Bogdanović B. Review: high temperature metal hydrides as heat storage materials for solar and related applications. Int J Mol Sci 2009;10:325–44.
[19] Stanmore BR, Gilot P. Review – calcination and carbonation of limestone during thermal cycling for CO_2 sequestration. Fuel Process Tech 2005;86:1707–43.
[20] Barker R. The reversibility of the reaction $CaCO_3 \leftrightarrow CaO + CO_2$. J Appl Chem Biotechnol 1973;23:733–42.
[21] Barker R. The reactivity of calcium oxide towards carbon dioxide and its use for energy storage. J Appl Chem Biotechnol 1974;24:221–7.
[22] Flamant G. Thermochimie solaire à hautes températures, résultats expérimentaux. Quelques perspectives d'application. Rev Phys Appl 1980;15:503–11.
[23] Badie JM, Bonet C, Faure M, Flamant G, Foro R, Hernandez D. Decarbonation of calcite and phosphate rock in solar chemical reactors. Chem Eng Sci 1980;35:413–20.
[24] Meier A, Bonaldi E, Cella GM, Lipinski W, Wuillemin D, Palumbo R. Design and experimental investigation of a horizontal rotary reactor for the solar thermal production of lime. Energy 2004;29:811–21.
[25] Foro R. Conception et caractérisation d'un réacteur solaire à lit fluidisé annulaire application à la décarbonatation, Thèse de doctorat, Université de Perpignan, France, 1981.
[26] Kyaw K, Kanamori M, Matsuda H, Hasatani M. Study of carbonation reactions of Ca–Mg oxides for high temperature energy storage and heat transformation. J Chem Eng Jpn 1996;29(1):112–8.
[27] Aihara M, Nagai T, Matsushita J, Negishi Y, Ohya H. Development of porous solid reactant for thermal-energy storage and temperature upgrade using carbonation/decarbonation reaction. Appl Energy 2001;69:225–38.
[28] Kato Y, Harada N, Yoshizawa Y. Kinetic feasibility of a chemical heat pump for heat utilization of high-temperature processes. Appl Therm Eng 1997;19:239–54.
[29] Kato Y, Saku D, Harada N, Yoshizawa Y. Utilization of high temperature heat from nuclear reactor using inorganic chemical heat pump. Prog Nucl Energy 1998;32(¾):563–70.
[30] Kato Y, Yamada M, Kanie T, Yoshizawa Y. Calcium oxide/carbon dioxide reactivity in a pack bed reactor of a chemical heat pump for high-temperature gas reactors. Nucl Eng Des 2001;210:1–8.
[31] Kato Y, Takahashi F, Sekiguchi T, Ryu J. Study on medium temperature chemical heat storage using mixed hydroxides. Int J Refrig 2009;32:661–6.
[32] Kato Y, Nakahata J, Yoshizawa Y. Durability characteristics of the hydration magnesium oxide under repetitive reaction. J Mater Sci 1999;34:475–80.
[33] Kato Y, Yamashita N, Kobayashi K, Yoshizawa Y. Kinetic study of the hydration of magnesium oxide for a chemical heat pump. Appl Therm Eng 1996;16(11):853–62.
[34] Kato Y, Takahashi F, Watanabe A, Yoshizawa Y. Thermal performance of a packed bed reactor of a chemical heat pump for cogeneration. Trans IChem 2000;78(Part A):745–8.
[35] Kato Y, Takahashi F, Yoshizawa Y, Watanabe A. Thermal analysis of a magnesium oxide water chemical heat pump for cogeneration. Appl Therm Eng 2001;21:1067–81.
[36] Kato Y, Sasaki Y, Yoshizawa Y. Magnesium oxide/water chemical heat pump to enhance energy utilization of cogeneration system. Energy 2005;30:2144–55.
[37] Kato Y, Saito T, Soga T, Ryu J, Yoshizawa Y. Durable reaction material development for magnesium oxide/water chemical heat pump. J Chem Eng Jpn 2007;40(13):1264–9.
[38] Ishitobi H, Hirao N, Ryu J, Kato Y. Dehydration and hydration behavior of metal-salt-modified materials for chemical heat pumps. Appl Therm Eng 2013;50:1639–44.
[39] Ishitobi H, Hirao N, Ryu J, Kato Y. Evaluation of heat output densities of lithium chloride-modified magnesium hydroxide for thermochemical energy storage. Ind Eng Chem Res 2013;52:5321–5.
[40] Halstead PE, Moore AE. The thermal dissociation of Calcium Hydroxide. J Chem Soc 1957:3873–5.
[41] Matsuda H, Ishizu T, Lee SK, Hasatani M. Kinetic study of $Ca(OH)_2$/CaO reversible thermochemical reaction for thermal energy storage by means of chemical reaction. Kagaku Kogaku Ronbunshu 1985;11:542–8.
[42] Kanamori M, Matsuda H, Hasatani M. Heat storing/releasing characteristics of a chemical heat storage unit of electricity using a $Ca(OH)_2$/CaO reaction. Heat Transfer – Jpn Res 1996;25(6):400–9 (, 1996).
[43] Ogura H, Shimojyo R, Kage H, Matsuno Y, Mujumdar AS. Simulation of hydration/dehydration of CaO/$Ca(OH)_2$ chemical heat pump reactor for cold/hot heat generation. Dry Technol 1999;17(7–8):1579–92.
[44] Fujimoto S, Bilgen E, Ogura H. CaO/$Ca(OH)_2$ chemical heat pump system. Energy Convers Manage 2002;43:947–60.
[45] Fujimoto S, Bilgen E, Ogura H. Dynamic simulation of CaO/$Ca(OH)_2$ chemical heat pump systems. Exergy 2002;2:6–14.
[46] Ogura H, Yamamoto T, Kage H. Efficiencies of CaO/H_2O/$Ca(OH)_2$ chemical heat pump for heat storing and heating cooling. Energy 2003;23:1479–93.
[47] Ogura H, Abliz S, Kage H. Studies on applicability of scallop material to calcium oxide/calcium hydroxide chemical heat pump. Fuel Process Technol 2004;85:1259–69.
[48] Kanzawa A, Arai Y. Thermal energy storage by chemical reaction, augmentation of heat transfer and thermal decomposition in the CaO/$Ca(OH)_2$ powder. Sol Energy 1981;27(4):289–94.
[49] Darkwa K. Thermochemical energy storage in inorganic oxides: an experimental evaluation. Appl Therm Eng 1998;18(6):387–400.
[50] Azpiazu MN, Morquillas JM, Vasquez A. Heat recovery from a thermal energy storage based on the $Ca(OH)_2$/CaO cycle. Appl Therm Eng 2003;23:733–41.
[51] Wereko-Brobby CY. Calcium hydroxide storage for solar thermal power generation systems. Colloque: le génie chimique et le stockage de l'énergie, 8–9 December 1980, p. 4-1–4-5.
[52] Brown DR, Lamarche JL, Spanner GE. Chemical energy storage system for SEGS solar thermal plant. BATELLE; 1991.
[53] Fujii I, Ishino M, Akiyama S, Murthy MS, Rajanandam KS. Behaviour of $Ca(OH)_2$/CaO pellet under dehydration and hydration. Sol Energy 1994;53(4):329–41.
[54] Schaube F, Wörner A, Tamme R. High temperature thermo-chemical heat storage for CSP using gas-solid reaction. SolarPACES, Perpignan, France; 21–24 September 2010.
[55] Schaube F, Wörner A, Tamme R. High temperature thermochemical heat storage for concentrated solar power using gas-solid reaction. J Sol Energy Eng 2011;133(3):031006-1–7.
[56] Schaube F, Koch L, Wörner A, Müller-Steinhagen H. A thermodynamic and kinetic study of the de and rehydration of $Ca(OH)_2$ at high H_2O partial pressures for thermo-chemical heat storage. Thermochem Acta 2012.
[57] Schaube F, Kohzer A, Schütz J, Wörner A, Müller-Steinhagen H. De- and rehydration of $Ca(OH)_2$ in a reactor with direct heat transfer for thermo-chemical heat storage. Part A: experimental results. Chem Eng Res Des 2012.
[58] Schaube F, Kohzer A, Schütz J, Wörner A, Müller-Steinhagen H. De- and rehydration of $Ca(OH)_2$ in a reactor with direct heat transfer for thermo-chemical heat storage. Part B: Validation model. Chem Eng Res Des 2013.
[59] Fahim MA, Ford JD. Energy storage using the BaO_2–BaO reaction cycle. Chem Eng J 1983;27:21–8.
[60] Bowrey RG, Jutsen J. Energy storage using the reversible oxidation of barium oxide. Sol Energy 1978;21:523–5.
[61] B. Wong, L. Brown, F. Schaube, R. Tamme, C. Sattler, Oxide based thermochemical heat storage, SolarPACES, Perpignan, France; 21–24 September 2010.
[62] Report final phase 2 DLR (2011), Solarpaces; 2012.
[63] Buckingham R, Wong B, Brown L, Sattler C, Schaube F, Wörner A. Metal oxide based thermochemical energy storage for concentrated solar power – thermodynamics and parasitic loads for packed bed reactors, SolarPACES, Granada, Spain; 20–23 September 2011.
[64] Neises M, Tescari S, De Oliveira L, Roeb M, Sattler C, Wong B. Solar-heated rotary kiln for thermochemical energy storage. Sol Energy 2012;86:3040–8.
[65] Temkin M, Pyzhev V. Kinetics of ammonia synthesis on promoted iron catalyst. Acta Physicochim URSS 1940;12(3):327–56.
[66] Lovegrove K, Luzzi A, Soldiani I, Kreetz H. Developing ammonia based thermochemical energy storage for dish power plants. Sol Energy 2004;76:331–7.
[67] Kreetz H, Lovegrove K. Theoretical analysis and experimental results of a 1 kWchem ammonia synthesis reactor for a solar thermochemical energy storage system. Sol Energy 1999;67:287–96.
[68] Carden PO. Energy corradiation using the reversible ammonia reaction. Sol Energy 1977;19:365–78.
[69] Williams OM, Carden PO. Energy storage efficiency for the ammonia/hydrogen–nitrogen thermochemical energy transfer system. Energy Res 1979;3:3–9.

[70] Lovegrove K. Thermodynamic limits on the performance of a solar thermochemical energy storage system. Int J Energy Res 1993;17:817–29.
[71] Lovegrove K. Exergetic optimisation of a solar thermochemical energy storage system subject to real constraints. Int J Energy Res 1993;17:831–45.
[72] Luzzi A, Lovegrove K, Filippi E, Fricker H, Schmitz-Goeb M, Chandapillai M, et al. Technico-economic analysis of a 10 MWe solar thermal power plant using ammonia-based thermochemical energy storage. Sol Energy 1999;66:91–101.
[73] Dunn R, Lovegrove K, Burgess G. Ammonia receiver design for a 500 m² dish. In: Proceedings of SolarPACES 2010, Perpignan, France; September 2010.
[74] Lovegrove K, Burgess G, Pye J. A new 500 m² paraboloidal dish solar concentrator. Sol Energy 2011;85:620–6.
[75] Dunn R, Lovegrove K, Burgess.G. A review of ammonia-based thermochemical energy storage for concentrating solar power. In: Proceeding of the IEEE; 2011.
[76] Ma Q, Luo L, Wang RZ, Sauce G. A review on transportation of heat energy over long distance: exploratory development. Renew Sust Energy Rev 2009;13:1532–40.
[77] Kugeler K, Niessen HF, Röth-Kamat M. Transport of nuclear heat by means of chemical energy (nuclear long distance energy). Nucl Energy Des 1975;34:65–72.
[78] Fedders H, Harth R, Höhlein B. Experiments for combing nuclear heat with the methane steam-reforming process. Nucl Eng Des 1975;34:119–27.
[79] Fedders H, Höhlein B. Operating a pilot plant circuit for energy transport with hydrogen rich gas. Int J Hydrog Energy 1982;7(10):793–800.
[80] Aristov YI, Parmon V, Cacciola G, Giordano N. High-temperature chemical heat pump based on reversible catalytic reactions of cyclohexane-dehydrogenation/benzene-hydrogenation: comparison of the potentialities of different flow diagrams. Int J Energy Res 1993;17:293–303.
[81] Edwards JH, Maitra AM. The chemistry of methane reforming with carbon dioxide and its current and potential applications. Fuel Process Technol 1995;42:269–89.
[82] Edwards JH, Do KT, Maitra AM. The use of solar-based CO_2/CH_4 reforming for reducing greenhouse effect gas emissions during the generation of electricity and process heat. Energy Convers Manage 1996;37(6-8):1339–44.
[83] Wörner A, Tamme R. CO_2 reforming of methane in a solar driven volumetric receiver-reactor. Catal Today 1998;46:165–74.
[84] Cacciola G, Anikeev V, Recupero V, Kirillov V, Parmon V. Chemical heat pump using heat of reversible catalytic reactions. Int J Energy Res 1987;11(4):519–29.
[85] Chubb TA. Analysis of gas dissociation solar thermal power system. Sol Energy 1975;17:129–36.
[86] Kunii D, Levenspiel O. Fluidization engineering. 2nd ed.. Boston: Butterworth-Heinemann; 1991.
[87] Lovegrove K, Luzzi A, Kreetz H. A solar-driven ammonia-based thermochemical energy storage system. Sol Energy 1999;67:309–16.
[88] Lovegrove K, Luzzi A, McCann M, Freitag O. Exergy analysis of ammonia-based solar thermochemical power systems. Sol Energy 1999;66(2):103–15.
[89] Kreetz H, Lovegrove K, Luzzi A. Maximizing thermal power output of an ammonia synthesis, reactor for a solar thermochemical energy storage system. J Sol Energy Eng 2001;123:75–82.